Blocken B, Janssen WD, van Hooff T. 2012. CFD simulation for pedestrian wind comfort and wind safety in urban areas: General decision framework and case study for the Eindhoven University campus. ***Environmental Modelling & Software*** 30: 15-34.

CFD simulation for pedestrian wind comfort and wind safety in urban areas: General decision framework and case study for the Eindhoven University campus

B. Blocken* [(a)], W.D. Janssen [(a)], T. van Hooff [(a,b)]

(a) Building Physics and Systems, Eindhoven University of Technology, P.O. box 513, 5600 MB Eindhoven, the Netherlands

(b) Division of Building Physics, Department of Civil Engineering, Katholieke Universiteit Leuven, Kasteelpark Arenberg 40, P.O. Box 2447, 3001 Leuven, Belgium

Research highlights:

- CFD is increasingly used for assessment of wind comfort and safety in urban areas
- Framework with integration of CFD best practice guidelines in iterative procedure
- Graphical representation of the framework by flow-chart including three cases
- Application for complex case study with grid-convergence analysis and validation
- Support and guidance for future studies of wind comfort and wind safety with CFD

Graphical abstract:

* **Corresponding author**: Bert Blocken, Building Physics and Systems, Eindhoven University of Technology, P.O.Box 513, 5600 MB Eindhoven, the Netherlands. Tel.: +31 (0)40 247 2138, Fax +31 (0)40 243 8595
E-mail address: b.j.e.blocken@tue.nl

Blocken B, Janssen WD, van Hooff T. 2012. CFD simulation for pedestrian wind comfort and wind safety in urban areas: General decision framework and case study for the Eindhoven University campus. ***Environmental Modelling & Software*** 30: 15-34.

CFD simulation for pedestrian wind comfort and wind safety in urban areas: General decision framework and case study for the Eindhoven University campus

B. Blocken* [(a)], W.D. Janssen [(a)], T. van Hooff [(a,b)]

(a) Building Physics and Systems, Eindhoven University of Technology, P.O. box 513, 5600 MB Eindhoven, the Netherlands

(b) Division of Building Physics, Department of Civil Engineering, Katholieke Universiteit Leuven, Kasteelpark Arenberg 40, P.O. Box 2447, 3001 Leuven, Belgium

Abstract

Wind comfort and wind safety for pedestrians are important requirements in urban areas. Many city authorities request studies of pedestrian wind comfort and wind safety for new buildings and new urban areas. These studies involve combining statistical meteorological data, aerodynamic information and criteria for wind comfort and wind safety. Detailed aerodynamic information can be obtained using Computational Fluid Dynamics (CFD), which offers considerable advantages compared to wind tunnel testing. However, the accuracy and reliability of CFD simulations can easily be compromised. For this reason, several sets of best practice guidelines have been developed in the past decades. Based on these guidelines, this paper presents a general simulation and decision framework for the evaluation of pedestrian wind comfort and wind safety in urban areas with CFD. As a case study, pedestrian wind comfort and safety at the campus of Eindhoven University of Technology are analysed. The turbulent wind flow pattern over the campus terrain is obtained by solving the 3D steady Reynolds-averaged Navier-Stokes equations with the realizable k-ε model on an extensive high-resolution grid based on grid-convergence analysis. The simulation results are compared with long-term and short-term on-site wind speed measurements. Wind comfort and wind safety are assessed and potential design improvements are evaluated. The framework and the case study are intended to support and guide future studies of wind comfort and wind safety with CFD and, this way, to contribute to improved wind environmental quality in urban areas.

Keywords: Computational Fluid Dynamics (CFD); wind flow; building aerodynamics; guidelines; discomfort and danger; built environment; experimental validation

1. Introduction

Urban areas should be designed to ensure the comfort, health and safety of their inhabitants and users. Wind comfort and wind safety for pedestrians are important requirements for urban areas. Although thermal comfort is also important (e.g. Stathopoulos 2006, Metje et al. 2008), wind comfort and safety generally only refer to the mechanical effects of wind on people (e.g., Lawson and Penwarden 1975, Willemsen and Wisse 2007). In particular near high-rise buildings, high wind velocities are often introduced at pedestrian level that can be experienced as uncomfortable or even dangerous. Uncomfortable wind conditions have proven detrimental to the success of new buildings (Durgin and Chock 1982). Wise (1970) reports about shops that are left untenanted because of the windy environment that discouraged shoppers. Lawson and Penwarden (1975) report dangerous wind conditions to be responsible for the death of two old ladies after being blown over by sudden wind gusts near a high-rise building. Many urban authorities nowadays recognize the importance of pedestrian wind comfort and wind safety and require such studies before granting building permits for new buildings or new urban areas.

Studies of wind comfort and wind safety involve combining statistical meteorological data with aerodynamic information and with wind comfort and wind safety criteria. The aerodynamic information is needed to transform the statistical meteorological data from the weather station (meteorological site) to the location of interest at the building site. At this location, the transformed statistical data are combined with the comfort and

* **Corresponding author**: Bert Blocken, Building Physics and Systems, Eindhoven University of Technology, P.O.Box 513, 5600 MB Eindhoven, the Netherlands. Tel.: +31 (0)40 247 2138, Fax +31 (0)40 243 8595
E-mail address: b.j.e.blocken@tue.nl

safety criteria to assess local wind comfort and safety. This procedure is schematically depicted in Figure 1. Wind statistics at the meteorological site can be expressed as potential wind speed (U_{pot}), i.e. corresponding to a terrain with aerodynamic roughness length $z_0 = 0.03$ m. The aerodynamic information usually consists of two parts: the terrain related contribution and the design related contribution. The terrain related contribution represents the change in wind statistics from the meteorological site to a reference location near the building site, i.e. the transformation of U_{pot} to U_0. The design related contribution represents the change in wind statistics due to the local urban design, i.e. the transformation of U_0 to the local wind speed U. Information on transformation procedures to determine terrain related contributions can be found in (e.g., Simiu and Scanlan 1986, Verkaik 2006). The design related contribution (i.e. the wind flow conditions around the buildings at the building site) can be obtained by either wind tunnel modelling or CFD. Wind comfort and safety criteria generally exist of a threshold value of the wind speed, and an allowed exceedance probability of this threshold. Tables 1 and 2 show the criteria for wind comfort and wind safety in the Dutch Wind Nuisance Standard NEN 8100 (NEN 2006a).

Considerable developments have been made in the past years concerning the determination of terrain related contributions (e.g. Verkaik 2000, 2006, NEN 2006b) and the comparison and evaluation of criteria for wind comfort and wind safety (e.g. Lawson and Penwarden 1975, Hunt et al. 1976, Penwarden et al. 1978, Murakami et al. 1980, Bottema 1993, 2000, Willemsen and Wisse 2002, 2007, NEN 2006a). As an example, in the Netherlands, these developments have been integrated in the Dutch Wind Nuisance Standard NEN 8100 (NEN 2006a) and the Dutch Practice Guideline NRP 6097 (NEN 2006b). To the best knowledge of the authors, this standard is the first wind nuisance standard in the world. The application of CFD in combination with these developments however is less established. Therefore, the simulation framework that is presented in this paper focuses on the accurate and reliable quantification of the design related contribution with CFD, however linked to the practical application of CFD for wind comfort and wind safety assessment.

CFD has some important advantages compared to wind tunnel testing. Wind tunnel measurements are generally only performed at a few selected points in the urban model, and do not provide a whole image of the flow field. CFD on the other hand provides whole-flow field data, i.e. data on the relevant parameters in all points of the computational domain. Unlike wind tunnel testing, CFD does not suffer from potentially incompatible similarity requirements because simulations can be conducted at full scale. This is particularly important for extensive urban areas such as the case study in this paper. CFD simulations easily allow parametric studies to evaluate alternative design configurations, especially when the different configurations are all a priori embedded within the same computational domain and grid (see e.g. van Hooff and Blocken 2010a).

Because of these advantages, CFD is increasingly used to study a wide range of wind environmental problems in urban areas, including urban air pollution (e.g. Canepa 2004, Meroney 2004, Chu et al. 2005, Hanna et al. 2006, Blocken et al. 2008a, Gromke et al. 2008, Mensink and Cosemans 2008, Yang and Shao 2008, Solazzo et al. 2009, Balczo et al. 2009, Gousseau et al. 2011a, 2011b, Tominaga and Stathopoulos 2011, Moonen et al. 2011), natural ventilation of buildings (e.g. Jiang and Chen 2002, Evola and Popov 2006, Chen 2009, van Hooff and Blocken 2010a, 2010b, Norton et al. 2010, van Hooff et al. 2011a), wind-driven rain on buildings (e.g. Choi 1993, Blocken and Carmeliet 2004, 2006, 2007, Huang and Li 2010, van Hooff et al. 2011b), convective heat transfer (e.g. Blocken et al. 2009, Defraeye et al. 2010, 2011a, 2011b, Defraeye and Carmeliet 2010, Karava et al. 2011, Saneinejad et al. 2011), wind erosion (e.g. Tominaga and Mochida 1999, Parsons et al. 2004, Hussein and El-Shishiny 2009, Tominaga et al. 2011), wind energy (e.g. Milashuk and Crane 2011) and other applications (e.g. Neofytou et al. 2006, Wakes et al. 2010). In the past, CFD has been frequently used to study wind speed conditions at pedestrian level in urban areas, but only very rarely has this information been used as part of complete wind comfort and wind safety studies. Examples of the application of CFD for pedestrian-level wind conditions can be found in (e.g. Murakami 1990, Gadilhe et al. 1993, Stathopoulos and Baskaran 1990, He and Song 1999, Yoshie et al. 2007, Blocken et al. 2007a, 2008b). While these studies did not assess wind comfort and wind safety, they are very valuable because they have evaluated CFD as an important ingredient of such studies. To the knowledge of the authors, wind comfort and wind safety studies based on CFD have only been published by Richards et al. (2002), Hirsch et al. (2002), Blocken et al. (2004), Blocken and Carmeliet (2008) and Blocken and Persoon (2009).

While the use of CFD for the evaluation of pedestrian wind conditions has long been an issue of debate (Stathopoulos 2002), in the past decade, strong support for its application has been provided by the establishment of several sets of best practice guidelines (BPG). Indeed, in CFD simulations, a large number of choices have to be made by the user. It is well known that these choices can have a very large impact on the results. In a typical CFD simulation, the user has to choose the approximate equations describing the flow (steady RANS, unsteady RANS (URANS), LES or hybrid URANS/LES), the level of detail in the geometrical representation of the buildings, the size of the computational domain, the type and resolution of the computational grid, the boundary conditions, the discretisation schemes, the initialisation data and the iterative convergence criteria. Important best practice guidelines have been developed and/or published by Casey and Wintergerste (2000), Menter et al. (2002), Franke et al. (2004, 2007, 2011), Scaperdas and Gilham (2004), Bartzis et al. (2004), Jakeman et al. (2006), Blocken et al. (2007b) and Tominaga et al. (2008). In this respect, it is important to note that the Dutch

Wind Nuisance Standard (NEN 2006a) explicitly allows the user to choose between wind tunnel experimentation and CFD to determine the design related contribution. This fact can be considered as a milestone in the acceptance process of CFD as a tool for the evaluation of wind comfort and wind safety in urban areas. However, it does not absolve the user from providing quality assurance. The decision to treat wind tunnel experimentation and CFD as *equals* in the Dutch standard has not been made lightly and has indeed led to the specification of quality assurance requirements in the standard, both for CFD and for wind tunnel testing. This reinforces the importance of BPG and their integration in wind comfort and wind safety studies.

The first objective of the present paper is to provide a framework for integration of the existing BPG into wind comfort and wind safety studies performed with CFD. To the knowledge of the authors, such a framework does not yet exist. The second objective of this paper is to apply this framework and the BPG to a complex case study, i.e. pedestrian wind comfort and safety at the campus of Eindhoven University of Technology. There is indeed a lack of detailed case studies based on the BPG, especially case studies in which the CFD simulations are validated with on-site measurements. As correctly stated by Willemsen and Wisse (2007), case studies are important as guidance and demonstration projects. In addition, they also provide valuable feedback to improve and refine the BPG guidelines.

In section 2, an overview of the current BPG for CFD in urban aerodynamics and pedestrian-level wind conditions is provided. The framework is presented in section 3. Section 4 introduces the case study of the Eindhoven University campus. In section 5, the on-site wind speed measurements for CFD validation are briefly outlined. The CFD geometry, grid, boundary conditions and solution parameters are described in section 6. Section 7 provides the grid-convergence analysis and the validation study, and section 8 completes the case study by combining the CFD data with the information in the Dutch wind nuisance standard. Sections 9 (discussion) and 10 (conclusions) conclude the paper.

2. Overview of best practice guidelines

2.1. Overview of best practice guideline documents

The BPG for CFD in urban aerodynamics originate from the pioneering studies in the late 70-ies and 80-ies. Typical investigations included the effects of the size of the computational domain, the grid resolution, the boundary conditions and the turbulence model on the computational results (e.g. Murakami and Mochida 1989, Baetke et al. 1990, Stathopoulos and Baskaran 1990, Cowan et al. 1997, Hall 1997). In addition, Schatzmann et al. (1997) provided an important contribution on validation with field and laboratory data (1997). These studies have provided a lot of valuable information. While these efforts were fragmented at first, in the past decade they have been combined and this has resulted in several extensive sets of BPG for the CFD simulation of environmental flows.

In 2000, the ERCOFTAC[1] Special Interest Group on Quality and Trust in Industrial CFD published an extensive set of BPG for industrial CFD users focused on RANS (Reynolds-averaged Navier-Stokes) simulations (Casey and Wintergerste 2000). Although they were not specifically intended for wind flow around buildings, many of these guidelines also apply for simulations of urban aerodynamics. Within the EC project ECORA[2], Menter et al. (2002) published BPG based on the ERCOFTAC guidelines, but modified and extended specifically for CFD code validation. Within QNET-CFD[3], the Thematic Area on Civil Construction and HVAC (Heating, Ventilating and Air-Conditioning) and the Thematic Area on the Environment presented some best practice advice for CFD simulations of wind flow and dispersion (Scaperdas and Gilham 2004, Bartzis et al. 2004).

In 2004, Franke et al. (2004) compiled a set of specific recommendations for the use of CFD in wind engineering from a detailed review of the literature, as part of the European COST[4] Action C14: Impact of Wind and Storm on City Life and Built Environment. Later, this contribution was extended into an extensive "Best Practice Guideline for the CFD simulation of flows in the urban environment" (Franke et al. 2007, 2011), in the framework of the COST Action 732: Quality Assurance and Improvement of Microscale Meteorological Models, managed by Schatzmann and Britter (http://www.mi.uni-hamburg.de/Home.484.0.html). Like the ERCOFTAC guidelines, also the COST 732 guidelines were primarily focused on steady RANS simulations, although also some information on URANS, LES and hybrid URANS/LES was provided.

In 2008, Tominaga et al. (2008) published the "AIJ guidelines for practical applications of CFD to pedestrian wind environment around buildings", and Tamura et al. (2008) wrote the "AIJ guide for numerical prediction of wind loads on buildings". These efforts of the Architectural Institute of Japan are based on extensive cross-

[1] ERCOFTAC = European Research Community on Flow, Turbulence and Combustion

[2] ECORA = Evaluation of Computational Fluid Dynamic Methods for Reactor Safety Analysis

[3] QNET-CFD = Network for Quality and Trust in the Industrial Application of CFD

[4] COST = European Cooperation in Science and Technology

comparisons between CFD simulation results and high-quality wind tunnel measurements to support the development of guidelines for practical CFD applications. The guidelines by Tominaga et al. (2008) focus on steady RANS simulations, while the guidelines by Tamura et al. (2008) also consider LES, given the importance of time-dependent analysis for wind loading of buildings and structures.

In 2006, Jakeman et al. (2006) published an important position paper describing ten iterative steps in the development and evaluation of environmental models, which also apply to CFD models.

These BPG documents have been based on more basic guidelines and standards concerning verification and validation, as outlined in e.g. Roache (1994, 1997), AIAA[5] (1998), Oberkampf et al. (2004), Roy (2005, 2010), ASME[6] (2009), and others. While in complex urban aerodynamics problems it is sometimes – due to computational constraints – not possible to adhere to all of these basic guidelines, they do provide the best practice in the field and underlie the more general BPG mentioned earlier. It is interesting to note that the importance of numerical accuracy control is emphasized by the Journal of Fluids Engineering Editorial Policy (ASME 2011), incited by contributions by Roache et al. (1986) and Freitas (1993), which demands at least formally second-order accurate spatial discretisation.

Apart from the general guidelines on CFD in urban aerodynamics mentioned above, also some very specific guidelines were published. These include (1) consistent modelling of equilibrium atmospheric boundary layers in computational domains and (2) high-quality grid generation. Consistent modelling of atmospheric boundary layer flow is important to avoid the unintended changes (called streamwise gradients or horizontal inhomogeneity) that can occur in the vertical profiles of mean wind speed and turbulence quantities as they travel from the inlet of the computational domain towards the modelled buildings (e.g. Richards and Hoxey 1993, Blocken et al. 2007a, 2007b, Franke et al. 2007, Hargreaves and Wright 2007, Yang et al. 2009, Gorle et al. 2009, Richards et al. 2011, Parente et al. 2011). This problem can dramatically affect the quality of the simulation results (Blocken et al. 2007a). Richards and Hoxey (1993) provided inlet profiles and wall boundary conditions that are consistent with the standard k-ε model for z_0-type wall functions, i.e. wall functions in which the aerodynamic roughness length z_0 is present as a roughness parameter. As many – commercial – CFD codes employ k_S-type wall functions, i.e. with the equivalent sand-grain roughness height k_S as a roughness parameter, Blocken et al. (2007b) derived the specific relationships between k_S and z_0, for Fluent 6 and Ansys CFX, and demonstrated the importance of satisfying these relationships in CFD simulations of wind flow around buildings (Blocken et al. 2007a). The NAFEMS[7] CFD Working Group published an introductory guide for grid and mesh generation for CFD (Tucker and Mosquera 2001). Based on this guide, van Hooff and Blocken (2010a) presented a body-fitted grid generation technique that allows the simultaneous generation of the computational geometry and a high-quality computational grid. As opposed to automatic and semi-automatic unstructured grid generation techniques, the technique in (van Hooff and Blocken 2010a) allows a strong degree of control over the size and shape of the computational cells. With this technique, rather complex geometries can be meshed, without resorting to the use of pyramidal and tetrahedral cells (van Hooff and Blocken 2010a; 2010b; van Hooff et al. 2011a; 2011b), which can be detrimental for convergence with higher-order discretisation schemes and therefore for computational accuracy.

The establishment of these guidelines has been an important step towards more accurate and reliable CFD simulations. Note that several of these guidelines have been developed specifically to support the evaluation of pedestrian-level wind conditions (Franke et al. 2004, Blocken et al. 2007a, Tominaga et al. 2008).

2.2. Some main aspects of the best practice guidelines

For an overview of the BPG, the reader is referred to the above-mentioned references. The intention of this section is to briefly highlight and explain some of the main elements of these guidelines that will be explicitly included in the framework presented in the next section.

- The computational geometry should contain all buildings and obstacles that have a significant effect on the flow at the location of interest. These should be modelled explicitly, i.e. with their main shape (Franke et al. 2004, 2007, Blocken et al. 2007b, Tominaga et al. 2008). Others can be modelled implicitly, but in this case specifying appropriate ground roughness boundary conditions is crucial (Blocken et al. 2007b).
- The computational domain should be large enough to avoid artificial acceleration of the flow. Its size can be based on the height of the tallest building in the urban configuration and/or on the blockage ratio (Franke et al. 2004, 2007, Tominaga et al. 2008).
- The computational grid should preferably consist of hexahedral or prismatic cells near solid boundaries, with cell faces perpendicular to the boundary (Casey and Wintergerste 2000, Franke et al. 2004, 2007, Tominaga et al. 2008). Even for many complex geometries, this can fairly easily be achieved by the grid generation

[5] AIAA = American Institute of Aeronautics and Astronautics

[6] ASME = American Society of Mechanical Engineers

[7] NAFEMS = National Agency for Finite Element Methods and Standards

technique by van Hooff and Blocken (2010a). The grid resolution should be based on a grid-sensitivity or grid-convergence analysis on at least three different grids (Casey and Wintergerste 2000; Franke et al. 2004, 2007, Tominaga et al. 2008). For uniform reporting of grid-convergence studies, using the grid-convergence index (GCI) of Roache (1994, 1997) is recommended.

- The boundary conditions should be consistent, i.e. the inflow, ground roughness and top boundary conditions should match and not yield excessive unintended streamwise gradients (e.g. Richards and Hoxey 1993, Blocken et al. 2007a, 2007b, Franke et al. 2007, Hargreaves and Wright 2007). Near-wall treatment is taken care of using wall functions. The standard wall functions by Launder and Spalding (1974) are most frequently used, although improved wall function formulations exist, e.g. the non-equilibrium wall functions by Kim and Choudhury (1995).
- First-order discretisation schemes should not be used due to the associated large amount of numerical diffusion (e.g. Franke et al. 2007, ASME 2011). At least formally second-order accurate discetisation schemes should be used. These however impose stronger demands on the quality of the computational grid. Computational grids with lower-quality cells, such as tetrahedral cells, might show convergence difficulties when combined with higher-order discretisation schemes.
- Iterative convergence should be monitored and should not be terminated without assurance that further iterations will not yield substantial changes in the flow variables of interest (e.g. Franke et al. 2007, Tominaga et al. 2008, ASME 2011).

Note that some best practice guidelines explicitly state that they give no best practice advice for the choice of turbulence models (e.g. Franke et al. 2007), while others advise the use of revised k-ε models and differential stress models instead of the often used standard k-ε model (Tominaga et al. 2008).

3. Simulation and decision framework for pedestrian wind comfort and safety in urban areas

This section only provides an overall or "high-level" simulation and decision framework based on the existing BPG. High-level refers to the fact that it is built upon and encompasses more basic (lower-level) and generic components, such as the BPG, which are in turn built upon the more basic guidelines in terms of verification and validation.

A distinction is made between three cases in which wind comfort and wind safety studies are required:

- Case 1: new developments within an existing urban configuration, for which on-site measurements are available or will be conducted;
- Case 2: new developments within an existing urban configuration, for which no on-site measurements are available or will be conducted;
- Case 3: development of a new urban configuration, for which – evidently – no on-site measurements are available during the design stage.

For new developments in existing urban areas, in general, one will like to compare the future level of wind comfort and wind safety with the present level. It is therefore recommended to evaluate both the existing and the new urban configuration with CFD. Whenever possible, on-site measurements should be made to provide validation data for the CFD simulations of the existing configuration (*Case 1*). The reason is that on-site measurements, in spite of their disadvantages, represent the complex reality without simplifications and are therefore the true validation data for numerical models. It is however important that these measurement are made during a sufficiently long measurement period (Schatzmann and Leitl 2011), as will be explained later. The on-site measurement data can also be used to calibrate the CFD simulations, which is especially important for the parameter "local roughness height of the ground surface of streets and squares" around the explicitly modelled buildings (see Blocken and Persoon 2009). If such measurements are not possible, an alternative validation procedure called "sub-configuration validation" can be employed (*Cases 2 and 3*). It consists of subdividing the actual configuration into a number of generic sub-configurations, each of which contains one or several of the main physical flow features that occur in the actual configuration (e.g. Oberkampf et al. 2004, Franke et al. 2007, Blocken and Carmeliet 2008). For generic sub-configurations, several high-quality experimental data sets are available in the published literature and/or online (e.g. the CEDVAL database of the University of Hamburg (www.mi.uni-hamburg.de/cedval), the data sets by the Architectural Institute of Japan (http://www.aij.or.jp/jpn/publish/cfdguide/index_e.htm) or the CODASC database of the University of Karlsruhe (http://www.ifh.uni-karlsruhe.de/science/aerodyn/CODASC.htm)), which are then used for CFD validation. When a given combination of computational parameters and settings provides accurate simulation results for each of the sub-configurations, it can reasonably be assumed that the same or a similar combination will also provide accurate results for the actual configuration.

The flowchart encompassing the three cases is shown in Figure 2, with sub-charts in Figures 3 and 4. It is briefly discussed below for each of the cases.

For Case 1, due to the availability of on-site measurements, a regular validation study can be conducted, as indicated by step "C" in the flowchart, which is further outlined in Figure 3. At first, on-site measurements are gathered (C1). In the simulations, a distinction is made between the selection of computational parameters that are well prescribed by existing BPG and those which are not (due to their inherent complexity). The domain size, computational grid, boundary conditions, discretisation schemes, algorithms for pressure interpolation and pressure-velocity coupling are all well prescribed by BPG, as mentioned in section 2.2. The extent to which the geometry is reproduced in the model, the choice of the turbulence model and of the type of wall functions are less well prescribed, because it is more difficult to provide general guidelines about these parameters. However, the available BPG information and experience with previous simulations can guide their selection. With these selected parameters ((C2) and (C3) in Figure 3), a first simulation is performed for the existing urban configuration. Next, a grid-convergence analysis is performed (C4): the grid is systematically coarsened and/or refined, and simulations on these new grids are performed. The results are compared until sufficient grid independence has been established. The most economical grid is the coarsest one that still provides sufficiently grid-independent results. For this grid, the Grid Convergence Index (GCI) (Roache 1994, 1997) should be determined and reported. The results on this grid are compared with the on-site measurements (C5). When insufficiently accurate results are obtained, increasing the level of geometrical detail of the model and/or selection of another turbulence model and/or other wall functions is necessary (C7). This could include switching from steady RANS to LES. Note that the definition of "sufficiently accurate" depends to some extent on the judgement and expectations of the modeller. When the CFD results are considered accurate enough (C6), the simulations are performed for at least 12 wind directions (0°, 30°, 60°, … 330°) (step "D" in Figure 2) and subsequently combined with the statistical meteorological data, the terrain-related transformation model and the comfort and safety criteria (E). This provides the level of wind comfort and safety for the existing urban configuration. When the new developments in this existing urban configuration do not incur major changes, the same computational parameters and settings can be used for the CFD simulations of this new urban configuration (G-H). When the new developments do incur major changes, a new validation study is necessary, which will be sub-configuration validation (L), which is outlined in Figure 4. Note that in terms of urban and building aerodynamics and validation, a design change can be considered "major" when it leads to major changes in the flow field, i.e. to the occurrence of new or additional flow features that require additional validation efforts. Finally, when the design is comfortable and safe, i.e. when the thresholds of mean wind speed and turbulence are not exceeded for a given period of time, the design with the new developments can be approved (I-K). If the design does not pass the comfort and/or safety criteria, communication with the urban planners and/or building developers is needed (J) to jointly and iteratively arrive at a new design configuration that can pass both criteria.

For Case 2 and Case 3, no on-site measurements are available. While it can also be useful to first evaluate wind comfort and safety in the existing configuration for Case 2, this is not included in the flowchart. The process starts with sub-configuration validation (step "L" in Figure 2; further outlined in Figure 4). When this has been successful, the computational geometry and grid of the new design configuration are constructed, a grid-convergence analysis is performed and the GCI is calculated (M in Figure 2). The CFD simulations are made for at least 12 wind directions (N) and wind comfort and safety are evaluated (H-I). Depending on the outcome of this evaluation, design changes might be needed (J). When these changes imply major changes that will yield different types of flow features (F), sub-configuration validation again has to be performed for these new geometrical configurations and flow features (L). If not, the CFD simulations for the new configuration can be performed based on the last sub-configuration validation study, after which wind comfort and safety are assessed. This procedure is repeated until a modified design is obtained that is comfortable and safe.

The CFD simulations are generally isothermal RANS simulations, but can also be LES simulations. Isothermal simulations are justified because the criteria for wind comfort and safety generally refer to high wind speed conditions (strong winds), in which mechanical turbulence generation dominates and thermal effects (including stratification) are small or absent.

In the next sections, a case study is presented that has been conducted with the presented framework. The case study involves the analysis of wind comfort and safety for a new development at the campus of Eindhoven University of Technology. This case study corresponds to Case 1: "developments within an existing urban configuration, for which on-site measurements are available or will be conducted".

4. Case study: campus of Eindhoven University of Technology (TU/e)

4.1. Buildings and surrounding environment

The TU/e campus covers an area of about 1.6 by 1.1 km (Fig. 5). All buildings at the campus are north-south oriented. The campus consists of high-rise and low-rise buildings. The highest buildings are the Vertigo building (VRT; 54.8 m), the Potentiaal building (PT; 54.8 m), the Main Building (HG; 45.4 m) and the TWE building

(33.2 m). One of the most important buildings on campus is the W-hall (Wh; Fig. 5, 6). It has a length of 148.8 m and a width of 74.4 m and it is surrounded by the high-rise buildings VRT, HG and PT. Outside the campus terrain, but in its immediate south-west vicinity, two other high-rise buildings are located: the Kennedy tower (82.8 m) and the Rabobank building (49.8 m). These buildings are not shown in Figs. 5 and 6 but will be included in the computational model.

Figure 7 shows the plan view of the wider surroundings with a radius of 10 km around the campus. The computational domain is indicated by the central white rectangle in the figure. This view with indication of the land use is needed to estimate the value of the aerodynamic roughness length z_0. Given the gradual development of internal boundary layers due to roughness changes, a 10 km fetch is required to determine z_0. This estimate is made for twelve wind direction sectors, based on the updated Davenport roughness classification (Wieringa 1992). These z_0 values are an important parameter in the inlet profiles of the CFD simulations.

4.2. Case study problem statement

As part of the master plan "Campus 2020", the TU/e campus will undergo a large redevelopment operation. The first part of this operation consists of the renovation of the W-hall. The new W-hall will become the highlight and the centre of the future Green Boulevard that runs from the west to the east side of the campus terrain and through the south part of the W-hall (Figs. 5 and 8). Figure 8a shows the original W-hall and Figure 8b shows the new design. The south part of this new design consists of a large roof-covered plaza with large entrances on the east and west side (entrance of 49.6 m length) and a small entrance on the south side (entrance of 12.4 m length) (Fig. 8b). The plaza will become the most important and central meeting place at the TU/e campus and it will host a wide variety of events such as meetings and parties. The new W-hall design also includes a new high-rise building (33.2 m) on top of the old construction (Fig. 8b). Given the importance of the plaza as a central meeting place, a good wind comfort is imperative. The concern for an inferior wind climate originates from the presence of several buildings on the campus with known wind discomfort issues, such as the area near the entrances of the Main Building (HG) and the entrance of the Vertigo Building (VRT). For this reason, a wind comfort study has to be performed to assess the current and future wind climate at the TU/e campus, and at the future W-hall plaza in particular. If necessary, remedial measures need to be suggested and evaluated.

The case to be assessed is that of the existing campus with the new W-hall design. On-site measurements have been performed to support the CFD wind comfort and safety study. This corresponds to Case 1 in section 3, i.e. new developments in an existing urban configuration with availability of on-site measurements. In the next section, the measurements are briefly outlined.

5. On-site measurements

Validation with experiments is an essential requirement for CFD studies in urban aerodynamics. For validation purposes, on-site wind speed measurements have been performed with 3D ultrasonic anemometers, indicated as step "C1" in Fig. 3. Their accuracy is < 1.5 RMS for wind incidence up to about 30° from the horizontal. Two types of measurements have been conducted: (1) measurements at three fixed positions for a period of 6 months (September 2009 - February 2010) and (2) measurements on 4 mobile posts (height 1.75 m) that were positioned at 12 different positions on windy days during the same period. The measurement positions are indicated in Fig. 9a. The fixed positions are position A at the top of the meteorological tower on the Auditorium building (reference position at 44.6 m height; Fig. 9b), position V at the northwest corner of the Vertigo building (at 5.4 m height; Fig. 9c) and position H on top of a camera mast at the south side of the Main Building (at 8.9 m height; Fig. 9d). Position A is the reference position in this study. It is the most exposed measurement position, although it is important to note that for easterly winds, the Main Building (45.4 m high) probably does provide some shelter. The measurement frequency at all positions is at least 1 Hz, and measurement data are averaged over 10 minutes to provide values of mean wind speed, wind direction and turbulence intensity. Only data with $U_{ref} > 4$ m/s are retained, in an attempt to exclude measurement values affected by thermal effects. This is important because these measurements will be used for CFD validation, and the CFD simulations will be performed for neutral atmospheric boundary layers and isothermal conditions (as required by the Dutch Standard NEN 8100). Note that the selected 4 m/s threshold is considered sufficiently high, but that this choice is also to some extent arbitrary, as the actual limit for neutral atmospheric flow in which mechanical turbulence overrides thermal turbulence depends on the interaction of a wide range of meteorological parameters including terrain roughness, insolation, atmospheric humidity, etc. The measurements with the mobile posts (Fig. 9e) had a duration of at least two hours and were performed outside office hours to minimize disturbances due to vehicle and pedestrian traffic. Data sets of wind speed and wind direction were obtained for a wide range of reference wind directions φ_A (i.e. at the reference measurement position A). Only data within the interval $[\varphi_A - 5; \varphi_A + 5]$ were attributed to a given wind direction φ_A. Data obtained at the fixed and the mobile

positions simultaneously were clustered in 6 groups corresponding to the following values for φ_A (in degrees clockwise from north): 24°, 109°, 182°, 215°, 262° and 318°. Additionally and in the same way, data obtained at the fixed positions for the 12 reference wind directions φ_A = 0° - 330° in 30° were clustered in 12 groups. The first 6 groups contain at most 18 measured values (10-min. averages). The number of measured values in the other 12 groups are indicated in Table 3. Note that all measurements with mobile posts were performed in winter conditions, i.e. without leaves on the deciduous trees present on the campus terrain. The CFD simulations will neglect the effect of the trees, therefore considering a worst-case situation. The measurement results will be presented along with the numerical results in section 7.

6. CFD simulations: computational model, domain, grid and solution parameters

6.1. Computational model and domain

All buildings on the TU/e campus are modelled explicitly, as well as the two additional adjacent high-rise buildings southwest of the campus (Kennedy tower and Rabobank building). To satisfy the BPG requirements for upstream and downstream domain length, different computational domains have been made for simulations with different wind directions. The upstream domain length is kept as short as possible to avoid the occurrence of unintended streamwise gradients (Blocken et al. 2007a, 2007b), while still satisfying the BPG by Franke et al. (2007) and Tominaga et al. (2008). The downstream domain length is taken long enough to allow the development of the wake region behind the buildings, which is beneficial for convergence of the simulations. The domain height, for all wind directions, is 830 m, which is 10 times the height of the highest building; i.e. the Kennedy tower. For wind directions 30° and 60° the domain dimensions are L x W x H = 2719 x 2257 x 830 m³. For wind directions 90°, 120° and 150° the domain dimensions are L x W x H = 2719 x 1838 x 830 m³. For wind directions 180°, 210°, 240° and 270° the domain dimensions are L x W x H = 2077 x 1838 x 830 m^3. For wind directions 300°, 330° and 360° the domain dimensions are L x W x H = 2077 x 2257 x 830 m^3.

6.2. Computational grid

Special care was given to the development of a high-quality and high-resolution grid that as much as possible satisfies the available BPG. The grid was constructed using the grid generation technique presented by van Hooff and Blocken (2010a), which allows a large degree of control over the quality of the grid and its individual cells. It consists of only hexahedral and prismatic cells and does not contain any tetrahedral or pyramid cells. Images of the grid of the campus terrain (with the old design of the W-hall), together with the corresponding photographs of the geometry, are shown in Figures 10 and 11. While generating this type of grid that has only hexahedral and prism cells requires a considerable effort, it avoids the well-known convergence problems that are associated with hybrid grids with tetrahedral cells, especially when the required second-order discretisation schemes are used. This advantage is considered very important, as first-order schemes should not be used due to their excessive contribution to numerical diffusion. This also corresponds to the guidelines by Franke et al. (2007), Tominaga et al. (2008) and ASME (2011), who also recommend or even demand using higher-order discretisation schemes.

The computational grid for this study consists of 7,554,091 cells for the case southwest wind direction. For other wind directions, slightly different total cell numbers are obtained. The grid is based on a grid-convergence analysis, as indicated in Fig. 3 (step "C4"). This analysis is performed for the prevailing southwest wind direction (215°) and is outlined in section 7.1. The smallest grid cell is 0.20 x 0.70 x 0.18 m^3, the largest is 70 x 70 x 120 m^3. In accordance with the BPG, five cell layers are provided below pedestrian height (1.75 m), at which the results will be evaluated. In the same grid, both the old and the new geometrical configuration of the W-hall were embedded, using the procedure by van Hooff and Blocken (2010a). In this way, generating the grid for the new configuration of the W-hall only requires deleting and adding a limited number of meshed volumes.

6.3. Boundary conditions

The neutral atmospheric boundary layer inflow at the inlet of the domain consists of the profiles of mean wind speed, turbulent kinetic energy and turbulence dissipation rate. The mean wind speed profile is prescribed by the logarithmic law with z_0 according to Fig. 7. The reference wind speed is 5 m/s at 10 m height. For z_0 = 0.5 m, the inlet longitudinal turbulence intensity (I_u) ranges from 29 % at pedestrian height (z = 1.75 m) to 5 % at gradient height. For z_0 = 1.0 m, I_u ranges from 39 % (z = 1.75 m) to 8 % at gradient height. The turbulent kinetic energy k is calculated using the longitudinal turbulence intensity (I_u) and assuming that the standard deviations of the turbulent fluctuations in the three directions are similar ($\sigma_u = \sigma_v = \sigma_w$): $k = 1.5(I_U.U)^2$. The inlet turbulence dissipation rate $\varepsilon = u^{*3}/(\kappa(z+z_0))$ where κ is the von Karman constant (0.42) and u^* is the friction velocity associated with the logarithmic wind speed profile.

At the outlet, zero static pressure is specified. At the sides and the top of the domain, symmetry boundary conditions are imposed (i.e. zero normal velocity and gradients). At the "walls", the standard wall functions by Launder and Spalding (1974) with the sand-grain roughness modification by Cebeci and Bradshaw (1977) are used. Within the domain, different types of "walls" or rough surfaces are distinguished, as indicated in Fig. 12: (1) Type 1: the building surfaces (facades and roofs), indicated in dark grey in Fig. 12; (2) Type 2: the ground surface of streets and parking areas between the buildings, indicated in light grey; (3) Type 3: the ground surface covered with grass, indicated in green; and (4) Type 4: the wider surroundings, that consist of buildings, trees and bushes. Note that the "type 4 buildings" are not modelled explicitly, i.e. they are not included in the domain with their real shape, but their effect on the flow is approximated by adjusted (increased) values for k_S and C_S. The reason is that they are located outside the area of interest and to limit the computational cost. The roughness parameters for each surface type are given in Fig. 12. The wall function inputs are the parameters k_S (equivalent sand-grain roughness height) and C_S (roughness constant). The relationship between the aerodynamic roughness length z_0 and the parameters k_S and C_S was derived by Blocken et al. (2007b). For Fluent 6.3, this relationship is $k_S = 9.793 z_0/C_S$. For surface types 2, 3 and 4, first the value of z_0 is estimated based on the updated Davenport-Wieringa roughness classification (Wieringa 1992). Next, k_S and C_S are determined to satisfy the equation $k_S = 9.793 z_0/C_S$. Note that in Fluent 6.3, the value of k_S is limited to the value of z_P, which is the height of the centre point of the wall-adjacent cell. When higher values can be specified, the code internally sets the value equal to z_P (without warning). Also note that for fully aerodynamically rough walls, which is the case in this study, only the product $k_S C_S$ is present in the wall function roughness modification. This allows circumventing the $k_S \leq z_P$ limitation by increasing C_S beyond its default value of 0.5 to specify larger roughness. The building surfaces (type 1) are given a roughness height $k_S = 0.1$ m and default roughness constant $C_S = 0.5$ to take into account the roughness of facades and roofs, such as profiles and other protrusions.

6.4. Other computational parameters

The CFD simulations are performed using the commercial CFD code Fluent 6.3.26 and the 3D steady RANS equations. Closure is provided by the realizable k-ε turbulence model (Shih et al. 1995). The choice for this turbulence model is based on the recommendations by Franke et al. (2004) and on earlier successful validation studies for pedestrian-level wind conditions (Blocken et al. 2004, 2007a, 2008b, Blocken and Carmeliet 2008, Blocken and Persoon 2009). Pressure velocity-coupling is taken care of by the SIMPLE algorithm. Pressure interpolation is second order. Second-order discretisation schemes are used for both the convection terms and viscous terms of the governing equations. For the comparisons with the measurements in this paper, simulations are performed for 18 reference wind directions: the 6 wind directions φ_A = 24°, 109°, 182°, 215°, 262°, 318° and the 12 wind directions φ_A = 0° - 330° in 30° intervals. For wind comfort assessment, only the simulations performed for the latter 12 wind directions will be used. The iterations were terminated when the scaled residuals (Fluent Inc. 2006) did not show any further reduction with increasing number of iterations. The following minimum values were reached: 10^{-8} for x-, y- and z-velocity, 10^{-7} for k and ε and 10^{-6} for continuity.

7. CFD simulations: results

7.1. Grid-convergence analysis

The grid-convergence analysis is indicated with label "C4" in Fig. 3. For the grid-convergence analysis, two additional grids have been constructed: a coarser grid with 2,598,602 cells and a finer grid with 12,392,255 cells (Fig. 13a-c). Simulations on these grids have been performed for the prevailing south-west wind direction (215°). Wind speed ratios are defined by dividing the local 3D velocity magnitude U by the 3D velocity magnitude at the reference location at the mast on the Auditorium building ($U_{ref,Aud}$). These ratios have been compared with each other. The comparisons have been made at the measurement positions and along two horizontal lines at pedestrian height (1.75 m), see Fig. 13d. Figs. 13e and f show that the differences between the coarse grid and the basic grid are significant, whereas the differences between the finer and basic grid are small. This seems to indicate that the basic grid is a good compromise between computational accuracy and computational cost. This grid is therefore selected for further analysis. The estimated fractional error on the basic grid (Roache 1994) or the basic-grid generalized Richardson error estimator (in comparing the basic grid to the fine grid) is E = 14%. The corresponding Grid Convergence Index GCI = 1.25*0.14 = 0.17.

7.2. CFD validation

The validation step is indicated with label "C5" in Fig. 3. The measured mean wind speed values are converted to wind speed ratios by division by the measured reference wind speed ($K_m = U_m/U_{A,m}$). The simulated

wind speed ratios are obtained by division of the simulated mean wind speed by the simulated reference wind speed ($K_{CFD} = U_{CFD}/U_{A,CFD}$).

Validation requires measurement data obtained from sufficiently long sampling periods (see e.g. Schatzmann and Leitl 2011). As mentioned earlier, the measurements at the three fixed positions (A, V, H) were made during 6 months, while those with the mobile measurement stations were only made during a few hours. Due to the short measurement period and the intrinsic variability of meteorological conditions, strictly, the data from the mobile stations can not serve as "validation data" (Schatzmann et al. 1997, Schatzmann and Leitl 2011). The measurements at the three fixed positions on the other hand can serve as validation data. Therefore, Fig. 14 compares the simulated and measured wind speed ratios at positions V and H (note that A is the reference position), for 12 reference wind directions. Also the standard deviation on the measurements is indicated. The figure shows a fair agreement at position V and a good agreement at position H. The average deviations are 25% and 11%, respectively. Note that the deviations at position V for wind from south to west are not surprising, given the very large wind speed gradients at this position and for these wind directions. In these cases, a small shift in location yields a large difference in wind speed ratio. Note that Fig. 14 shows no data for east wind directions (90°), because no measurements with $U_{ref,Aud} > 4$ m/s and $85° < \varphi_A < 95°$ occurred during the measurement period. Fig. 15 shows the difference between the simulated and measured local wind directions θ at positions V and H, for the 12 different reference wind directions φ_A. The average deviations are 21° and 22°, which is considered a good agreement. Only at one reference wind direction for every measurement position, the deviation is larger than 60°.

A comparison of simulated and measured wind speed ratios and wind directions at all 15 measurement positions (mobile and fixed positions) and for two reference wind directions (φ_A = 215° and 318°) is shown in Fig. 16. The black vectors show the measured (10-min. averaged) wind speed ratio vectors and the two additional black lines indicate the standard deviation of the wind directions. The magenta/grey vectors show the simulated wind speed ratios and wind directions. This figure also shows filled contours of the simulated wind speed ratio at pedestrian height, i.e. 1.75 m above ground level. The wind flow pattern at pedestrian level between the buildings is quite complex with large local gradients in wind speed and wind direction. Overall, a fair agreement between simulations and measurements is observed, although locally, significant deviations are present. These deviations are attributed to three main reasons: (1) the limited number of data samples at the mobile measurement positions (max. 18 10-min.values), which is not sufficient to "remove" the intrinsic meteorological variability from the measured averages (Schatzmann et al. 1997, Schatzmann and Leitl 2011); (2) the comparison of point values in regions of high velocity gradients, by which a small shift in location can yield a large change in local wind speed ratio and local wind direction; and (3) the fact that steady RANS has been found to provide quite accurate results (10-20% accuracy) in regions of high wind speed ratios, but to significantly underestimate wind speed in regions of lower wind speed ratios. This observation corresponds to previous detailed validation studies, as mentioned in a recent overview paper (Blocken et al. 2011). A possible reason for this observation is that regions with high wind speed ratios are generally characterized by lower turbulence intensities and lower wind direction fluctuations, and can therefore be better described by the statistically steady RANS approach for the turbulent flow.

Comparisons between CFD simulations and measurements have also been performed for other wind directions (not shown in figures). The overall accuracy, averaged over all measurement positions and wind directions, is 14%. This is considered a good agreement. However, it should be noted again that only the comparison with the long-term measured data in Fig. 14 and 15 can be considered validation.

In Figure 3, the results of this validation and comparison exercise imply that the simulations are considered sufficiently accurate (step "C6" in Fig. 3), and that the same level of geometrical representation and the same physical models can be retained for the remaining CFD simulations in this case study.

8. Assessment of wind comfort and wind safety

Wind comfort assessment in this case study is performed with the Dutch standard for wind comfort and wind safety. This standard was recently developed (NEN 2006a, 2006b) based on extensive research work by Verkaik (2000, 2006), Willemsen and Wisse (2002, 2007), Wisse and Willemsen (2003), Wisse et al. (2007), and others. It contains an improved and verified transformation model for the terrain related contribution (see section 1) that can provide the wind statistics at every location in the Netherlands, however without including the local building aerodynamic effects, which are part of the so-called design related contribution. Based on the wind statistics, Figure 17a shows the frequency distribution of the hourly mean wind speed for the position of the Eindhoven University campus. Figure 17b shows the distribution of the exceedance probability of the 5 m/s threshold at pedestrian height of 1.75 m, which was obtained by converting the data given by the transformation model from 60 m height to pedestrian height by assuming an aerodynamic roughness length $z_0 = 0.03$ m for a grass-covered open field. The sum of these exceedance probabilities over all wind directions is 7.7%. It is stressed that the data

in Figures 17a and 17b do not take into account the local effects of the buildings at the building site. These effects have to be included based on the CFD simulations.

As mentioned before, the standard explicitly allows the user to choose between wind tunnel testing and CFD to determine the design related contribution. In this standard, the comfort criterion has a threshold in the mean wind speed U_{THR} = 5 m/s for all types of activities. Depending on the type of activity and the maximum allowed discomfort probability, the code defines fives grades of wind comfort A–E (see Table 1, Willemsen and Wisse 2007). For the new plaza, grade A is required, which implies P < 2.5%. The safety criterion has a threshold U_{THR} = 15 m/s and a maximum allowed exceedance probability of 0.3%. To determine the exceedance probability, three steps have to be taken for each of the 12 wind directions.

(1) Obtain wind speed ratios ($\gamma = U/U_{ref,60m}$) from the CFD simulations. The reference wind speed value ($U_{ref,60m}$) is the value of the inlet wind speed profile at a height of 60 m. Note that this wind speed ratio differs from the wind speed ratio used for the validation and comparison of the CFD simulations with the measurements in the previous section;
(2) Convert threshold wind speed at pedestrian level to a threshold wind speed at a height of 60 m ($U_{THR,60m} = U_{THR}/\gamma$);
(3) Determine the percentage of time that the threshold value for the hourly mean wind speed at 60 m is exceeded according to the wind statistics of Eindhoven. These wind statistics for the 12 wind directions are provided by the Dutch Practice Guideline NPR 6097.

The total discomfort probability is the sum of the probabilities for the 12 wind directions, and is indicated in Figure 18a for the existing configuration (old W-hall design). The new design does not involve major design changes. Indeed, the addition of the high-rise construction and the open plaza do not give rise to specific flow features that would require additional validation studies. Therefore, the same settings can be used for the CFD simulations of the new configuration (see steps “G” and “H” in Fig. 2). This results in Figure 18c. Figures 18b and d illustrate the corresponding quality classes. The following conclusions are made:

(1) The discomfort probability contours and the comfort class contours are to a large extent determined by the discomfort probabilities for south-west wind direction, because this is the prevailing wind direction, and also the wind direction for which the strongest winds occur.
(2) The wind comfort study clearly indicates the known wind discomfort problem areas in the open areas (passages) under the HG building (see also Fig. 11) and around the corner of the VRT and HAL buildings. NEN 8100 indicates that these areas have a moderate wind climate for traversing, but a poor wind climate for strolling and sitting.
(3) The largest part of the campus has a good wind climate for traversing and a good to moderate wind climate for strolling.
(4) Wind comfort locally deteriorates south of the W-hall (old design) due to a jet emerging from the passage between the MA and HE building and entering the plaza through the south entrance. For the new design, this jet enters the roof-covered plaza, causing a moderate to poor wind climate for sitting. This implies that the design can not be approved and design changes/remedial measures are needed (step “J” in Fig. 2).

The most straightforward measure would be to close the south entrance. However, this was not an option in the design. Other straightforward remedial measures include moving the south entrance to left or right to avoid the entrance of the jet. Therefore, simulations are performed with different positions of the south entrance. Figure 19 shows four alternative configurations, where the gray framed squares show the roof pattern while the red lines represent the walls around the plaza. Option 1 consists of widening the entrance (to 49.6 m). For the other three options the entrance remains 12.4 m wide but it is moved to either the east or west side. This way the entrance is no longer at the same line as the passage between the buildings Matrix (MA) and Helix (HE). As these options do not involve major design changes, no additional validation studies are required (Fig. 2). Therefore, the same settings are again used to perform CFD simulations for the twelve wind direction sectors (step “G” in Fig. 2) and wind comfort and safety are assessed (step “H”). These calculations show that moving the south entrance 24.8 m to the east (option 2) is the best option for wind comfort on the square. The exceedence probability for wind nuisance for this configuration and the associated quality classes are shown in Figure 20. The assessment of wind safety indicates that the threshold of 0.05 % (see Table 2) is not exceeded for any position on the campus terrain, both in the old and the new configuration. As a result, the new design is both comfortable and safe and can therefore be approved.

9. Discussion

This paper has presented a general simulation and decision framework for the evaluation of pedestrian wind comfort and wind safety in urban areas with CFD. It was motivated by the increasing use of CFD for this type of problems. This is illustrated, for example, by the recent Dutch wind nuisance standard that explicitly allows the choice between either wind tunnel measurements or CFD. The framework is based on the Best Practice

Guidelines (BPG) that have been developed in the past decade. Some important comments need to be made concerning the applicability and limitations of this framework.

The framework does not prescribe the approximate form of the governing equations that should be used: steady RANS, Unsteady RANS (URANS), Large Eddy Simulation (LES) or hybrid URANS/LES. While LES is potentially more accurate than steady RANS, it is also much more time-consuming. The case study in this paper was based on steady RANS. This choice is supported by three reasons:

- The existing BPG have mostly been developed for steady RANS (e.g. Casey and Wintergerste 2000, Franke et al. 2004, 2007, Blocken et al. 2007b, Tominaga et al. 2008);
- Several authors have indicated that LES might still be too time-consuming for practical application in pedestrian-level wind environment studies (e.g. Yoshie et al. 2007);
- A recent literature review (Blocken et al. 2011) indicated that steady RANS is fairly accurate (10-20%) for the high wind speed regions, but not for the low wind speed regions (deviations up to factor 5). This does not necessarily mean that steady RANS is not accurate for wind comfort studies, because in such studies, generally only the high wind speed regions are of interest, and only high wind speeds contribute to the exceedance probability of the discomfort threshold of wind speed (i.e. 5 m/s in the Dutch Standard). However, care is needed when using criteria in which the discomfort threshold is much lower, such as the criteria by Isyumov and Davenport (1975) and Lawson (1978).

The Dutch wind nuisance standard applied in this study applies a comfort criterion that only includes the mean wind speed. Many other criteria use a linear combination of the mean wind speed and the standard deviation of the turbulent fluctuations (see e.g. the review by Bottema 2000). This way, gustiness, which can be important for wind comfort and wind safety, is explicitly included in the criteria. More research is needed to address the capabilities and deficiencies of steady RANS modelling in predicting not only mean wind speed but also turbulence intensities in urban areas.

In the present study, the effects of vegetation have not been taken into account. It is generally recognized that vegetation has a positive effect on wind comfort and wind safety (e.g. Mochida and Lun 2008), therefore neglecting vegetation is justified when attempting to assess a worst-case scenario, as was done in this study. CFD modelling of vegetation effects is not straightforward and is the subject of ongoing investigations (e.g. Mochida and Lun 2008, Gromke et al. 2008, Melese Endalew et al. 2009a, 2009b, Balczo et al. 2009).

CFD studies of urban aerodynamics generally involve quite complex geometries and large computational grids, as was also the case in this study. For such studies, grid-convergence analysis and validation with experiments are often very time-consuming, which may inhibit their application in practical cases when time and resources are limited. In principle, every new study should be accompanied by a grid-convergence analysis and by validation. However, when this is not possible, the grid resolution should at least be based on previous and similar studies that included a grid-convergence analysis. And the choice of the physical models (turbulence models etc.) should at least be based on previous and similar studies in which these models were successfully validated. These requirements are supported by the following quote by Ferziger (1993):

"… the frequently heard argument 'any solution is better than none' can be dangerous in the extreme. The greatest disaster one can encounter in computation is not instability or lack of convergence but results that are simultaneously good enough to be believable but bad enough to cause trouble."

Finally, some comments are made about validation and decisions in the simulation and decision framework. Validation is a very important ingredient of the framework. However, the required quality and the quantity of the experimental data and the required agreement between experiments and simulations for a validation exercise to be considered as "sufficient" are important issues of debate. Furthermore, while some of the decisions in the framework are clear and unambiguous, others are not, such as the answer to the question in step "F" in Figure 2: "Does the new design involve major changes?" and the answer to the question in step "C6" in Figure 3 and step "L7" in Figure 4: "Are the simulations sufficiently accurate?". These problems confirm that the framework and the best practice guidelines should always be applied in combination with the common sense and expert judgement of the modeller and with knowledge of the scientific literature. In spite of these remaining problems, it can be stated that the simulation and decision framework presented in this paper and the existing best practice guidelines provide a solid basis for CFD simulation for wind comfort and wind safety in urban areas.

10. Summary and conclusions

This paper has presented a simulation and decision framework for the evaluation of pedestrian wind comfort and wind safety in urban areas with CFD. In the past decades, CFD has been increasingly used to assess pedestrian-level wind conditions in urban areas. This increasing use is supported by the establishment of several sets of best practice guidelines (BPG). The calculated pedestrian-level wind conditions can be combined with statistical meteorological data, other aerodynamic information and with wind comfort and wind safety criteria to assess wind comfort and wind safety.

This paper has provided a framework for integration of the existing BPG into wind comfort and wind safety studies performed with CFD. An important component of the framework is the iterative procedure to arrive at new urban configurations that are comfortable and safe. Other important components are the basic ingredients of any CFD study such as grid-convergence analysis and validation with experiments. In the framework, a distinction has been made between three cases: (i) Case 1: new developments within an existing urban configuration, for which on-site measurements are available or will be conducted; (ii) Case 2: new developments within an existing urban configuration, for which no on-site measurements are available or will be conducted; and (iii) Case 3: development of a new urban configuration, for which – evidently – no on-site measurements are available during the design stage. A flowchart has been presented that encompasses the three cases. It outlines the basic steps to be followed in assessing – and if necessary, improving – wind comfort and wind safety.

Next, the developed framework and the BPG have been applied to a complex case study, i.e. pedestrian wind comfort and safety at the campus of Eindhoven University of Technology. This application was motivated by the lack of detailed case studies based on the BPG, especially case studies in which the CFD simulations are validated with on-site measurements. In the case study, the turbulent wind flow pattern over the campus terrain has been obtained by solving the 3D steady Reynolds-averaged Navier-Stokes equations with the realizable k-ε model on an extensive high-resolution grid. The grid has been based on a grid-convergence analysis with three different grids. The simulation results have been compared with on-site wind speed measurements. The average deviations at two fixed measurement positions were 25% and 11%, and the overall average deviation between simulated and measured wind speed was 14% on average, which is considered a good agreement. The deviations are at least partly caused by the deficiencies of steady RANS modelling and by the large wind speed gradients at many of the measurement positions. Wind comfort and wind safety have been assessed using the Dutch wind nuisance standard and various alternative design configurations have been evaluated, one of which provides a high quality of wind comfort at the roof-covered plaza.

The framework and the case study in this paper are intended to support and guide future studies of wind comfort and wind safety with CFD and, this way, to contribute to improved wind environmental quality in urban areas.

Acknowledgements

The authors thank the anonymous reviewers for many valuable comments that have improved the manuscript.

The numerical simulations reported in this paper were supported by the laboratory of the Unit Building Physics and Systems (BPS) of Eindhoven University of Technology.

References

AIAA, 1998. Guide for the verification and validatino of computational fluid dynamics simulations, American Institute of Aeronautics and Astronautics, AIAA, AIAA-G-077-1998, Reston, VA.

ASME, 2009. Standard for verification and validation in Computational Fluid Dynamics and heat transfer. ASME V&V 20-2009, The American Society of Mechanical Engineers.

ASME, 2011. http://journaltool.asme.org/Templates/JFENumAccuracy.pdf. Retrieved on 30 July 2011.

Baetke, F., Werner, H. and Wengle, H., 1990. Numerical simulation of turbulent flow over surface-mounted obstacles with sharp edges and corners. J. Wind Eng. Ind. Aerodyn. 35(1-3), 129-147.

Balczo, M., Gromke, C., Ruck, B., 2009. Numerical modeling of flow and pollutant dispersion in street canyons with tree planting. Meteorol. Z. 18(2), 197-206.

Bartzis, J.G., Vlachogiannis, D., Sfetsos, A., 2004. Thematic area 5: Best practice advice for environmental flows. The QNET-CFD Network Newsletter 2(4), 34-39.

Blocken, B., Roels, S., Carmeliet, J., 2004. Modification of pedestrian wind comfort in the Silvertop Tower passages by an automatic control system. J. Wind Eng. Ind. Aerodyn. 92 (10), 849-873.

Blocken, B., Carmeliet, J., 2004. A review of wind-driven rain research in building science. J. Wind Eng. Ind. Aerodyn. 92(13), 1079-1130.

Blocken, B., Carmeliet, J., 2006. The influence of the wind-blocking effect by a building on its wind-driven rain exposure. J. Wind Eng. Ind. Aerodyn. 94(2), 101-127.

Blocken, B., Carmeliet, J., 2007. Validation of CFD simulations of wind-driven rain on a low-rise building. Build. Environ. 42(7): 2530-2548.

Blocken, B., Carmeliet, J., Stathopoulos, T., 2007a. CFD evaluation of the wind speed conditions in passages between buildings – effect of wall-function roughness modifications on the atmospheric boundary layer flow. J. Wind Eng. Ind. Aerodyn. 95(9-11), 941-962.

Blocken, B., Stathopoulos, T., Carmeliet, J. 2007b. CFD simulation of the atmospheric boundary layer: wall function problems, Atmos. Environ. 41(2), 238-252.

Blocken, B., Carmeliet, J., 2008. Pedestrian wind conditions at outdoor platforms in a high-rise apartment building: generic sub-configuration validation, wind comfort assessment and uncertainty issues. Wind Struct. 11(1), 51-70.
Blocken, B., Stathopoulos T, Saathoff, P., Wang, X., 2008a. Numerical evaluation of pollutant dispersion in the built environment: comparisons between models and experiments. J. Wind Eng. Ind. Aerodyn. 96(10-11), 1817-1831.
Blocken, B., Stathopoulos, T., Carmeliet, J., 2008b. A numerical study on the existence of the Venturi-effect in passages between perpendicular buildings. J. Eng. Mech. 134(12), 1021-1028.
Blocken, B., Persoon, J., 2009. Pedestrian wind comfort around a large football stadium in an urban environment: CFD simulation, validation and application of the new Dutch wind nuisance standard. J. Wind Eng. Ind. Aerodyn. 97(5-6), 255-270.
Blocken, B., Defraeye, T., Derome, D., Carmeliet, J., 2009. High-resolution CFD simulations of forced convective heat transfer coefficients at the facade of a low-rise building. Build. Environ. 44(12), 2396-2412.
Blocken, B., Stathopoulos T, Carmeliet, J., Hensen, J.L.M., 2011. Application of CFD in building performance simulation for the outdoor environment: an overview. J. Building Perform. Simul. 4(2), 157-184.
Bottema, M., 1993. Wind climate and urban geometry. PhD thesis, Eindhoven University of Technology, 212 p.
Bottema, M., 2000. A method for optimisation of wind discomfort criteria. Build. Environ. 35(1), 1-18.
Canepa, E., 2004. An overview about the study of downwash effects on dispersion of airborne pollutants. Environ. Modell. Softw. 19(12), 1077-1087.
Casey, M., Wintergerste, T., 2000. Best Practice Guidelines, ERCOFTAC Special Interest Group on Quality and Trust in Industrial CFD, ERCOFTAC, Brussels.
Cebeci, T., Bradshaw, P., 1977. Momentum transfer in boundary layers, Hemisphere Publishing Corporation, New York.
Chen, Q., 2009. Ventilation performance prediction for buildings: A method overview and recent applications. Build. Environ. 44(4), 848-858.
Choi, E.C.C., 1993. Simulation of wind-driven rain around a building. J. Wind Eng. Ind. Aerodyn. 46&47, 721-729.
Chu, A.K.M., Kwok, R.C.W., Yu, K.N., 2005. Study of pollution dispersion in urban areas using Computational Fluid Dynamics (CFD) and Geographic Information System (GIS). Environ. Modell. Softw. 20(3), 273-277.
Cowan, I.R., Castro, I.P., Robins, A.G., 1997. Numerical considerations for simulations of flow and dispersion around buildings, J. Wind Eng. Ind. Aerodyn. 67 & 68, 535-545.
Defraeye, T., Blocken, B., Carmeliet, J., 2010. CFD analysis of convective heat transfer at the surfaces of a cube immersed in a turbulent boundary layer. Int. J. Heat Mass Transfer 53(1-3), 297-308.
Defraeye, T., Carmeliet, J. 2010. A methodology to assess the influence of local wind conditions and building orientation on the convective heat transfer at building surfaces. Environ. Modell. Softw. 25(12), 1813-1824.
Defraeye, T., Blocken, B., Carmeliet, J., 2011a. Convective heat transfer coefficients for exterior building surfaces: Existing correlations and CFD modelling. Energy Convers. Manage. 52(1), 512-522.
Defraeye, T., Blocken, B., Carmeliet, J., 2011b. An adjusted temperature wall function for turbulent forced convective heat transfer for bluff bodies in the atmospheric boundary layer. Build. Environ. 46(11), 2130-2141.
Durgin, F.H., Chock, A.W., 1982. Pedestrian wind levels: a brief review. Journal of the Structural Division ASCE 108 ST8, 1751–1767.
Evola, G., Popov, V., 2006. Computational analysis of wind driven natural ventilation in buildings. Energy Build. 38(5), 491-501.
Ferziger, J.H., 1993. Estimation and reuduction of numerical error. FED Vol. 158, Symposium on Quantification of Uncertainty in Computational Fluid Dynamics, ASME Fluid Engineering Division, Summer Meeting, Washington DC, June 20-24, pp. 1-8.
Fluent Inc., 2006. Fluent 6.3 User's Guide. Fluent Inc., Lebanon.
Franke, J., Hirsch, C., Jensen, A.G., Krüs, H.W., Schatzmann, M., Westbury, P.S., Miles, S.D., Wisse, J.A., Wright, N.G. 2004. Recommendations on the use of CFD in wind engineering. Proc. Int. Conf. Urban Wind Engineering and Building Aerodynamics, (Ed. van Beeck JPAJ), COST Action C14, Impact of Wind and Storm on City Life Built Environment, von Karman Institute, Sint-Genesius-Rode, Belgium, 5 - 7 May 2004.
Franke, J., Hellsten, A., Schlünzen, H., Carissimo, B., 2007. Best practice guideline for the CFD simulation of flows in the urban environment. COST 732: Quality Assurance and Improvement of Microscale Meteorological Models.
Franke, J., Hellsten, A., Schlünzen, H., Carissimo, B., 2011. The COST 732 best practice guideline for CFD simulation of flows in the urban environment – A summary. Int. J. Environ. Pollut. 44(1-4): 419-427.
Freitas, C.J., 1993. J. Fluids Eng. editorial policy statement on the control of numerical accuracy. J. Fluids Eng. 115, 339-340.

Gadilhe, A., Janvier, L., Barnaud, G., 1993. Numerical and experimental modelling of the three-dimensional turbulent wind flow through an urban square. J. Wind Eng. Ind. Aerodyn. 46-47, 755-763.
Gorlé, C., van Beeck, J., Rambaud, P., Van Tendeloo, G., 2009. CFD modelling of small particle dispersion: the influence of the turbulence kinetic energy in the atmospheric boundary layer. Atmos. Environ. 43(3), 673-681.
Gousseau, P., Blocken, B., Stathopoulos, T., van Heijst, G.J.F., 2011a. CFD simulation of near-field pollutant dispersion on a high-resolution grid: a case study by LES and RANS for a building group in downtown Montreal. Atmos. Environ. 45(2), 428-438.
Gousseau, P., Blocken, B., van Heijst, G.J.F., 2011b. CFD simulation of pollutant dispersion around isolated buildings: On the role of convective and turbulent mass fluxes in the prediction accuracy. J. Hazard. Mater. 194: 422-434.
Gromke, C., Buccolieri, R., Di Sabatino, S., Ruck B., 2008. Dispersion study in a street canyon with tree planting by means of wind tunnel and numerical investigations - Evaluation of CFD data with experimental data. Atmos. Environ. 42(37), 8640-8650.
Hall, R.C. (Ed.), 1997. Evaluation of modelling uncertainty. CFD modelling of near-field atmospheric dispersion. Project EMU final report, European Commission Directorate–General XII Science, Research and Development Contract EV5V-CT94- 0531, WS Atkins Consultants Ltd., Surrey.
Hanna, S.R., Brown, M.J., Camelli, F.E., Chan, S.T., Coirier, W.J., Hansen, O.R., Huber, A.H., Kim S., Reynolds R.M., 2006. Detailed simulations of atmospheric flow and dispersion in downtown Manhattan. An application of five computational fluid dynamics models. Bull. Am. Meteorol. Soc. 87, 1713-1726.
Hargreaves, D.M., Wright, N.G., 2007. On the use of the k–ε model in commercial CFD software to model the neutral atmospheric boundary layer. J. Wind Eng. Ind. Aerodyn. 95(5), 355-369.
He, J., Song, C.C.S., 1999. Evaluation of pedestrian winds in urban area by numerical approach. J. Wind Eng. Ind. Aerodyn. 81, 295–309.
Hirsch, C., Bouffioux, V., Wilquem, F., 2002. CFD simulation of the impact of new buildings on wind comfort in an urban area. Workshop Proceedings, Cost Action C14, Impact of Wind and Storm on City Life and Built Environment, Nantes, France.
Huang, S.H., Li, Q.S., 2010. Numerical simulations of wind-driven rain on building envelopes based on Eulerian multiphase model. J. Wind Eng. Ind. Aerodyn. 98(12), 843-857.
Hunt, J.C.R., Poulton, E.C., Mumford, J.C., 1976. The effects of wind on people: new criteria based upon wind tunnel experiments, Build. Environ. 11, 15–28.
Hussein A.S., El-Shishiny, H. 2009. Influences of wind flow over heritage sites: A case study of the wind environment over the Giza Plateau in Egypt, Environ. Modell. Softw. 24(3), 389-410.
Isyumov, N., Davenport, A.G., 1975. The ground level wind environment in built-up areas. In: Proceedings of Fourth International Conference on Wind Effects on Buildings and Structures. Heathrow, UK, Cambridge University Press, 403-422.
Jakeman, A.J., Letcher, R.A., Norton, J.P., 2006. Ten iterative steps in development and evaluation of environmental models. Environ. Modell. Softw. 21(5), 602-614.
Jiang, Y., Chen, Q., 2002. Effect of fluctuating wind direction on cross natural ventilation in buildings from large eddy simulation. Build. Environ. 37(4), 379-386.
Karava, P., Jubayer, C.M., Savory, E., 2011. Numerical modelling of forced convective heat transfer from the inclined windward roof of an isolated low-rise building with application to Photovoltaic/Thermal systems. Appl. Therm. Eng. 31(11-12), 1950-1963.
Kim, S-E., Choudhury, D., 1995. A near-wall treatment using wall functions sensitized to pressure gradient, ASME FED Vol. 217, Separated and Complex Flows.
Launder, B.E., Spalding, D.B., 1974. The numerical computation of turbulent flows. Comput. Meth. Appl. Mech. Eng. 3, 269-89.
Lawson, T.V., Penwarden, A.D., 1975. The effects of wind on people in the vicinity of buildings, Proceedings 4th International Conference on Wind Effects on Buildings and Structures, Cambridge University Press, Heathrow, pp. 605–622.
Lawson, T.V., 1978. The wind content of the built environment. J. Ind. Aerodyn. 3, 93-105.
Melese Endalew, A., Hertog, M., Gebreslasie Gebrehiwot, M., Baelmans, M., Ramon, H., Nicolai, B.M., Verboven, P., 2009a. Modelling airflow within model plant canopies using an integrated approach. Comput. Electron. Agric. 66(1): 9-24.
Melese Endalew, A., Hertog, M., Delele, M.A., Baetens, K., Persoons, T., Baelmans, M., Ramon, H., Nicolai, B.M., Verboven, P., 2009b. CFD modelling and wind tunnel validation of airflow through plant canopies using 3D canopy architecture. Int. J. Heat Fluid Flow 30(2): 356-368.
Mensink, C., Cosemans, G., 2008. From traffic flow simulations to pollutant concentrations in street canyons and backyards. Environ. Modell. Softw. 23(3), 288-295.

Menter, F., Hemstrom, B., Henrikkson, M., Karlsson, R., Latrobe, A., Martin, A., Muhlbauer, P., Scheuerer, M., Smith, B., Takacs, T., Willemsen, S., 2002. CFD Best Practice Guidelines for CFD Code Validation for Reactor-Safety Applications, Report EVOLECORA-D01, Contract No. FIKS-CT-2001-00154, 2002.

Meroney, R.N., 2004. Wind tunnel and numerical simulation of pollution dispersion: a hybrid approach. Working paper, Croucher Advanced Study Insitute on Wind Tunnel Modeling, Hong Kong University of Science and Technology, 6-10 December, 2004, 60 pp.

Metje, N., Sterling, M., Baker, C.J., 2008. Pedestrian comfort using clothing values and body temperatures. J. Wind Eng. Ind. Aerodyn. 96(4), 412-435.

Milashuk, S., Crane, W.A., 2011. Wind speed prediction accuracy and expected errors of RANS equations in low relief inland terrain for wind resource assessment purposes. Environ. Modell. Softw. 26(4): 429-433.

Mochida, A., Lun, I.Y.F., 2008. Pedestrian wind environment and thermal comfort at pedestrian level in urban area. J. Wind Eng. Ind. Aerodyn. 96, 1498-1527.

Moonen, P., Dorer, V., Carmeliet, J., 2011. Evaluation of the ventilation potential of courtyards and urban street canyons using RANS and LES. J. Wind Eng. Ind. Aerodyn. 99(4), 414-423.

Murakami, S., Uehara, K., Deguchi, K., 1980. Wind effects on pedestrians: new criteria based on outdoor observation of over 2000 persons, Proceedings of the 5th International Conference on Wind Engineering, Fort Collins, Colorado, pp. 277–288.

Murakami, S., Mochida, A., 1989. Three-dimensional numerical simulation of turbulent flow around buildings using the k−ε turbulence model. Build. Environ. 24 (1), 51-64.

Murakami, S., 1990. Computational wind engineering. J. Wind Eng. Ind. Aerodyn. 36(1), 517-538.

Murakami, S., 1993. Comparison of various turbulence models applied to a bluff body. J. Wind Eng. Ind. Aerodyn. 46&47, 21-36.

NEN, 2006a. Wind comfort and wind danger in the built environment, NEN 8100 (in Dutch) Dutch Standard.

NEN, 2006b. Application of mean hourly wind speed statistics for the Netherlands, NPR 6097:2006 (in Dutch). Dutch Practice Guideline.

Neofytou, P., Venetsanos, A.G., Vlachogiannis, D., Bartzis, J.G., Scaperdas, A., 2006. CFD simulations of the wind environment around an airport terminal building. Environ. Modell. Softw. 21(4), 520-524.

Norton, T., Grant, J., Fallon, R., Sun, D.W., 2010. Optimising the ventilation configuration of naturally ventilated livestock buildings for improved indoor environmental homogeneity. Build. Environ. 45(4), 983-995.

Oberkampf, W.L., Trucano, T.G., Hirsch, C., 2004. Verification, validation, and predictive capability in computational engineering and physics. Appl. Mech. Rev. 57(5), 345-384.

Parente, A., Gorlé, C., van Beeck, J., Benocci, C., 2011. Improved k-ε model and wall function formulation for the RANS simulation of ABL flows. J. Wind Eng. Ind. Aerodyn. 99(4), 267-278.

Parsons, D.R., Wiggs, G.F.S., Walker I.J., Ferguson, R.I., Garvey B.G., 2004. Numerical modelling of airflow over an idealised transverse dune. Environ. Modell. Softw. 19(2), 153-162.

Penwarden, A.D., Grigg, P.F., Rayment, R., 1978. Measurements of wind drag on people standing in a wind tunnel, Build. Environ. 13, 75–84.

Roache, P.J., Chia, K.N., White, F., 1986. Editorial policy statement on the control of numerical accuracy. J. Fluids Eng. 108:2

Roache, P.J., 1994. Perspective: a method for uniform reporting of grid refinement studies. J. Fluids Eng. 116, 405-413.

Roache, P.J., 1997. Quantification of uncertainty in computational fluid dynamics. Annu. Rev. Fluid Mech. 29, 123-160.

Richards, P.J., Hoxey, R.P., 1993. Appropriate boundary conditions for computational wind engineering models using the k-ε turbulence model. J. Wind Eng. Ind. Aerodyn. 46&47, 145-153.

Richards, P.J., Mallison, G.D., McMillan, D., Li, Y.F., 2002. Pedestrian level wind speeds in downtown Auckland. Wind Struct. 5(2-4), 151-164.

Richards, P.J., Norris, S.E., 2011. Appropriate boundary conditions for computational wind engineering models revisited. J. Wind Eng. Ind. Aerodyn. 99(4), 257-266.

Roy, C.H., 2005. Review of code and solution verification procedures for computational simulation. J. Comput. Phys. 205, 131-156.

Roy, C.H., 2010. Review of discretization error estimators in scientific computing.48th AIAA Aerospace Sciences Meeting Including the New Horizons Forum and Aerospace Exposition, 4-7 January 2010, Orlando, Florida.

Saneinejad, S., Moonen, P., Defraeye, T., Carmeliet, J., 2011. Analysis of convective heat and mass transfer at the vertical walls of a street canyon. J. Wind Eng. Ind. Aerodyn. 99(4), 424-433.

Scaperdas, A., Gilham, S., 2004. Thematic Area 4: Best practice advice for civil construction and HVAC, The QNET-CFD Network Newsletter 2(4), 28-33.

Schatzmann, M., Rafailidis, S., Pavageau, M., 1997. Some remarks on the validation of small-scale dispersion models with field and laboratory data. J. Wind Eng. Ind. Aerodyn. 67-68, 885-893.
Schatzmann, M., Leitl, B., 2011. Issues with validation of urban flow and dispersion CFD models. J. Wind Eng. Ind. Aerodyn. 99(4), 169-186.
Shih, T.H., Liou, W.W., Shabbir, A., Zhu, J., 1995. A new k-ε eddy-viscosity model for high Reynolds number turbulent flows – model development and validation. Comput. Fluids 24(3), 227-238.
Simiu, E., Scanlan, R.H., 1986. Wind effects on structures. An introduction to wind engineering, Second Ed. Wiley, New York.
Solazzo, E., Cai, X., Vardoulakis, S., 2009. Improved parameterisation for the numerical modelling of air pollution within an urban street canyon. Environ. Modell. Softw. 24(3), 381-388.
Stathopoulos, T., Baskaran, A., 1990. Boundary treatment for the computation of 3D turbulent conditions around buildings. J. Wind Eng. Ind. Aerodyn. 35: 177–200.
Stathopoulos, T., 2002. The numerical wind tunnel for industrial aerodynamics: real or virtual in the new millennium? Wind Struct. 5(2–4), 193–208.
Stathopoulos, T., 2006. Pedestrian level winds and outdoor human comfort. J. Wind Eng. Ind. Aerodyn. 94(11), 769-780.
Tamura, T., Nozawa, K., Kondo, K., 2008. AIJ guide for numerical prediction of wind loads on buildings. J. Wind Eng. Ind. Aerodyn. 96(10-11), 1974-1984.
Tominaga, Y., Mochida, A., 1999. CFD prediction of flowfield and snowdrift around a building complex in a snowy region. J. Wind Eng. Ind. Aerodyn. 81(1-3): 273-282.
Tominaga, Y., Mochida, A., Yoshie, R., Kataoka, H., Nozu, T., Yoshikawa, M., Shirasawa, T., 2008. AIJ guidelines for practical applications of CFD to pedestrian wind environment around buildings. J. Wind Eng. Ind. Aerodyn. 96(10-11), 1749-1761.
Tominaga, Y., Stathopoulos, T., 2011. CFD modeling of pollution dispersion in a street canyon: Comparison between LES and RANS. J. Wind Eng. Ind. Aerodyn. 99(4): 187-198.
Tominaga, Y., Okaze, T., Mochida, A., 2011. CFD modeling of snowdrift around a building: An overview of models and evaluation of a new approach. Build. Environ. 46: 899-910.
Tucker, P.G., Mosquera, A., 2001. NAFEMS introduction to grid and mesh generation for CFD. NAFEMS CFD Working Group, R0079, 56 pp.
van Hooff, T., Blocken, B., 2010a. Coupled urban wind flow and indoor natural ventilation modelling on a high-resolution grid: A case study for the Amsterdam ArenA stadium. Environ. Modell. Softw. 25 (1), 51-65.
van Hooff, T., Blocken, B., 2010b. On the effect of wind direction and urban surroundings on natural ventilation of a large semi-enclosed stadium. Comput. Fluids 39, 1146-1155.
van Hooff, T., Blocken, B., Aanen, L., Bronsema, B., 2011a. A venturi-shaped roof for wind-induced natural ventilation of buildings: wind tunnel and CFD evaluation of different design configurations. Build. Environ. 46(9), 1797-1807.
van Hooff, T., Blocken, B., van Harten, M., 2011b. 3D CFD simulations of wind flow and wind-driven rain shelter in sports stadia: influence of stadium geometry. Build. Environ. 46(1), 22-37
Verkaik, J.W., 2000. Evaluation of two gustiness models for exposure correction calculations. J. Appl. Meteorol. 39(9), 1613-1626.
Verkaik, J.W., 2006. On wind and roughness over land. PhD thesis. Wageningen University. The Netherlands, 123 p.
Wakes, S.J., Maegli, T., Dickinson, K.J., Hilton, M.J., 2010. Numerical modelling of wind flow over a complex topography. Environ. Modell. Softw. 25(2), 237-247.
Wieringa, J., 1992. Updating the Davenport roughness classification. J. Wind Eng. Ind. Aerodyn. 41-44, 357-368.
Willemsen, E., Wisse, J.A., 2002. Accuracy of assessment of wind speed in the built environment. J. Wind Eng. Ind. Aerodyn. 90, 1183-1190.
Willemsen, E., Wisse, J.A., 2007. Design for wind comfort in The Netherlands: Procedures, criteria and open research issues. J. Wind Eng. Ind. Aerodyn. 95(9-11), 1541-1550.
Wise, A.F.E., 1970. Wind effects due to groups of buildings, Proceedings of the Royal Society Symposium Architectural Aerodynamics, Session 3, Effect of Buildings on the Local wind, London. pp. 26–27 February.
Wisse, J.A., Willemsen, E., 2003. Standardization of wind comfort evaluation in the Netherlands. 11th Int. Conf. Wind Eng. (11ICWE), Lubbock, Texas.
Wisse, J.A., Verkaik, J.W., Willemsen, E., 2007. Climatology aspects of a wind comfort code, 12th Int. Conf. Wind Eng. (12ICWE), Cairns, Australia.
Yang, Y., Shao, Y., 2008. Numerical simulations of flow and pollution dispersion in urban atmospheric boundary layers. Environ. Modell. Softw. 23(7), 906-921.

Yang, Y., Gu, M., Chen, S., Jin, X., 2009. New inflow boundary conditions for modelling the neutral equilibrium atmospheric boundary layer in computational wind engineering. J. Wind Eng. Ind. Aerodyn. 97(2), 88-95.

Yoshie, R., Mochida, A., Tominaga, Y., Kataoka, H., Harimoto, K., Nozu, T., Shirasawa, T., 2007. Cooperative project for CFD prediction of pedestrian wind environment in the Architectural Institute of Japan. J. Wind Eng. Ind. Aerodyn. 95(9-11), 1551-1578.

TABLES

Table 1: Criteria for wind nuisance according to NEN 8100 (2006a)

$P(U_{THR} > 5$ m/s (in % hours per year)	Grade	Activity		
		Traversing	Strolling	Sitting
< 2.5	A	Good	Good	Good
2.5 – 5.0	B	Good	Good	Moderate
5.0 – 10	C	Good	Moderate	Poor
10 – 20	D	Moderate	Poor	Poor
> 20	E	Poor	Poor	Poor

Table 2: Criteria for wind danger according to NEN 8100 (2006a)

$P(U_{THR} > 15$ m/s (in % hours per year)	Grade	Activity		
		Traversing	Strolling	Sitting
0.05 - 0.30	Limited risk	Acceptable	Not acceptable	Not acceptable
≥ 0.30	Dangerous	Not acceptable	Not acceptable	Not acceptable

Table 3: Number of measurement samples (10-min. averaged) for the 12 reference wind directions

Ref. wind direction φ_A	0°	30°	60°	90°	120°	150°	180°	210°	240°	270°	300°	330°
Number of 10-min. values	166	304	6	0	317	32	520	529	431	205	61	77

FIGURES

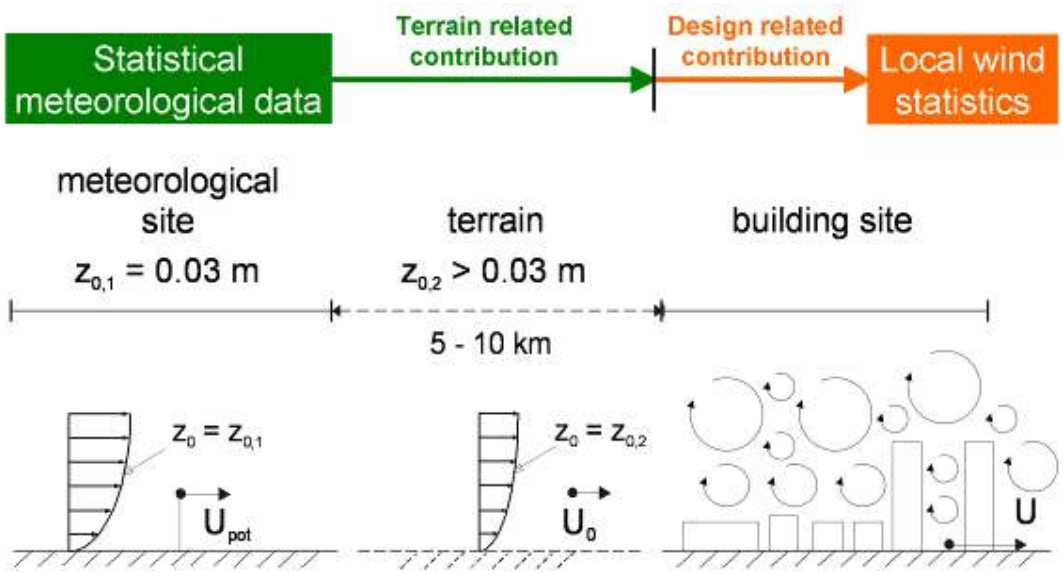

Figure 1. Schematic representation of transformation of statistical meteorological data from the meteorological site to the building site, with indication of the wind speed at the meteorological station (U_{pot}), the reference wind speed at the building site (U_0) and the wind speed at the location of interest (U). The corresponding aerodynamic roughness lengths z_0 are also indicated.

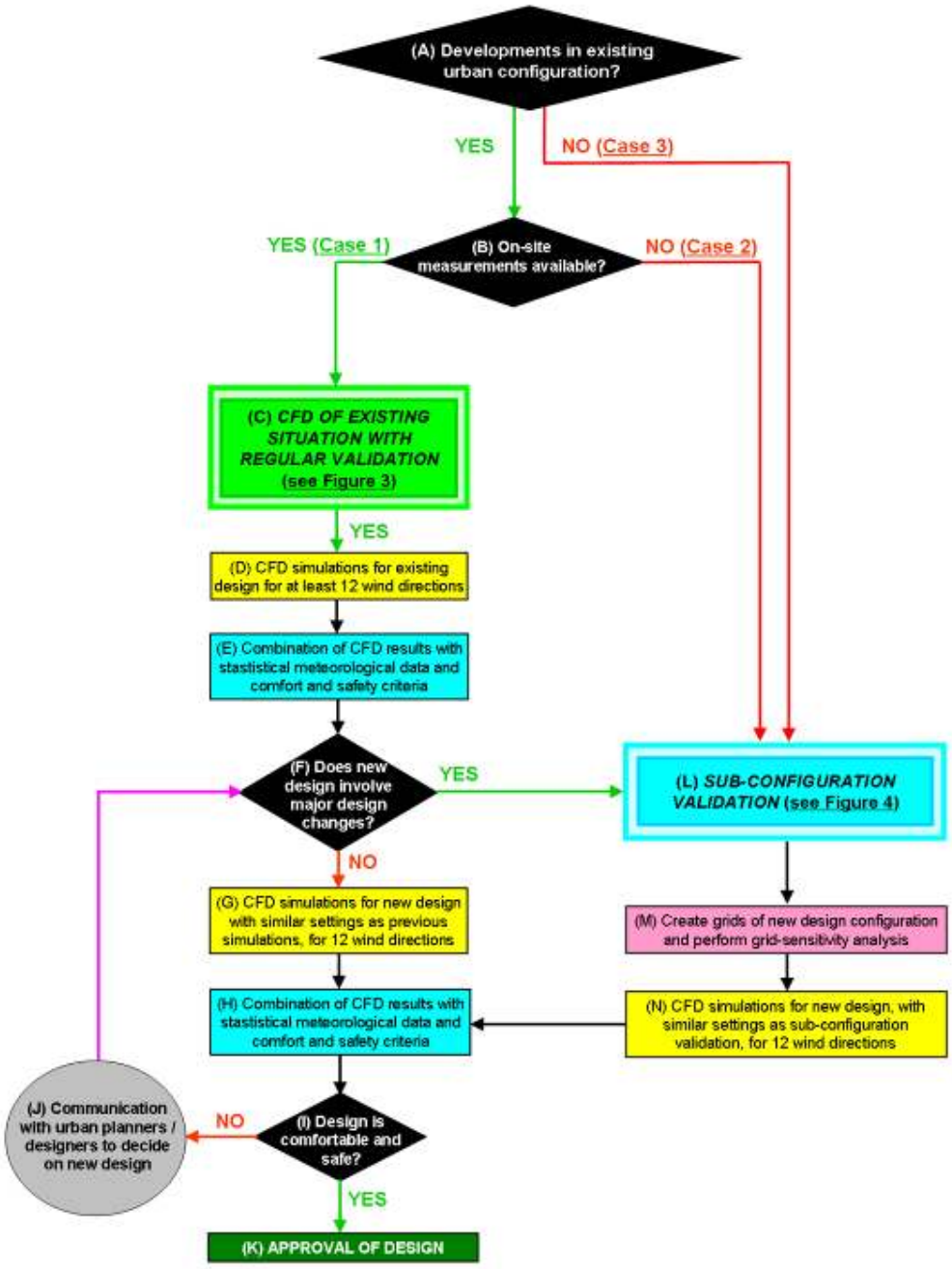

Figure 2. Flowchart illustrating the framework for the assessment of pedestrian wind comfort and safety with CFD. Part "C" and "L" are further outlined in Figures 3 and 4, respectively.

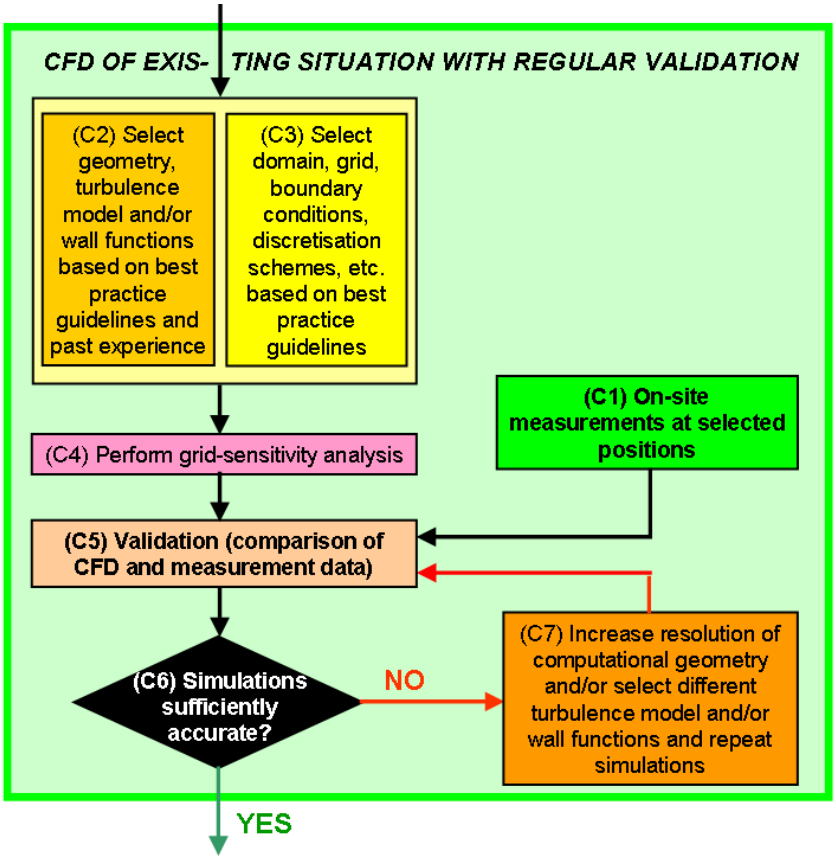

Figure 3. Flowchart outlining part "C" of the large flowchart in Figure 2.

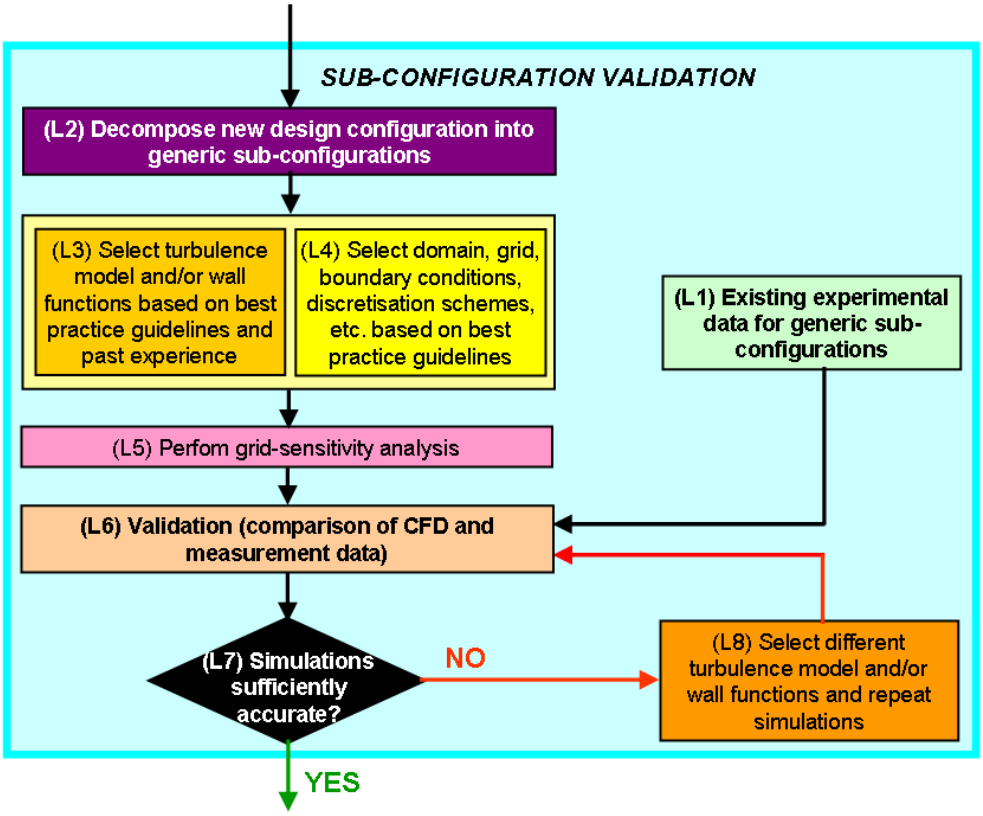

Figure 4. Flowchart outlining part "L" of the large flowchart in Figure 2.

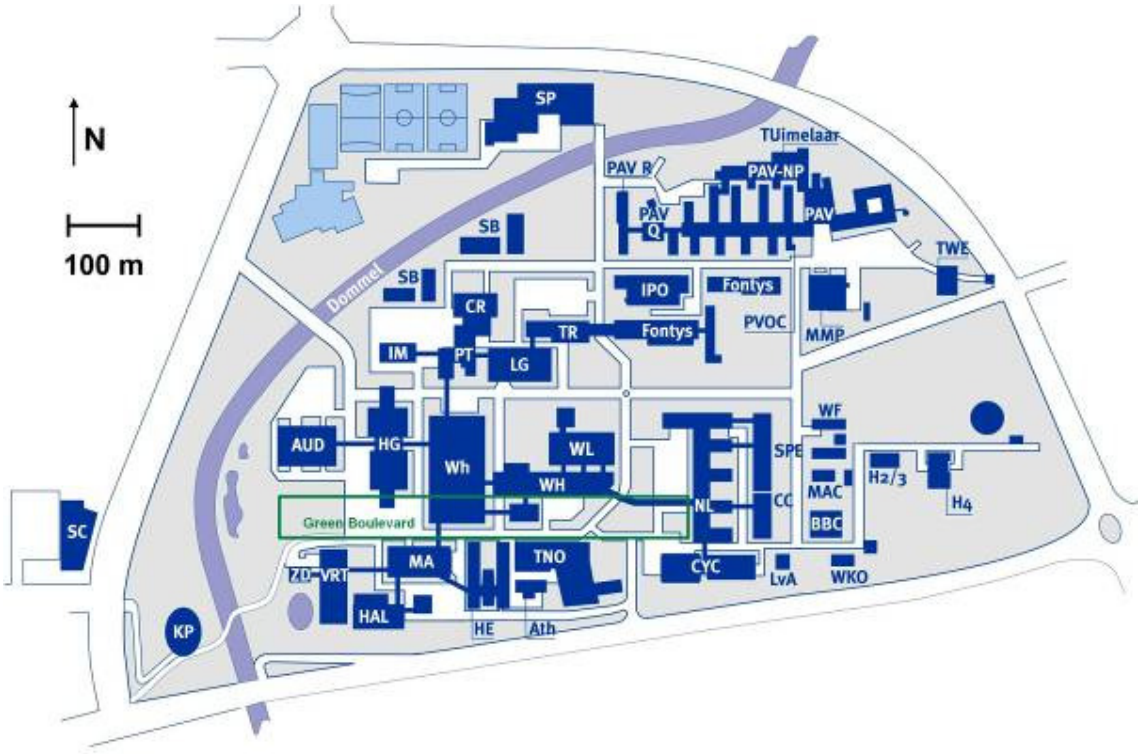

Ath	8.2 m	Fontys	15.2 m	LvA	7.4 m	PT	54.8 m	TWE	33.2 m
AUD	16.2 m	HAL	11.2 m	LG	7.5 m	SB	9.4 m	VRT	54.8 m
BBC	5 m	HE	24.1 m	MA	11.3 m	SPE	15.2 m	WF	3 m
CC	19.4 m	HG	45.4 m	MAC	5.3 m	SP	12 m	Wh	9.5 m
CR	12.3 m	IM	9.1 m	MMP	9.4 m	TNO	23.8 m	WH	18.2 m
CYC	8.5 m	IPO	15.2 m	NL	12 m	TR	15.2 m	WL	10.1 m
H2, H3, H4	5 m	KP	29 m	PAV	5 m	PAV-NP	3.5 m	ZD	12 m

Figure 5. Overview of buildings at the campus of Eindhoven University of Technology (TU/e). For every building, the average building height is indicated.

Figure 6. Photograph of the largest part of the TU/e campus with indication of abbreviated building names. The photograph also indicates the presence and location of deciduous vegetative elements.

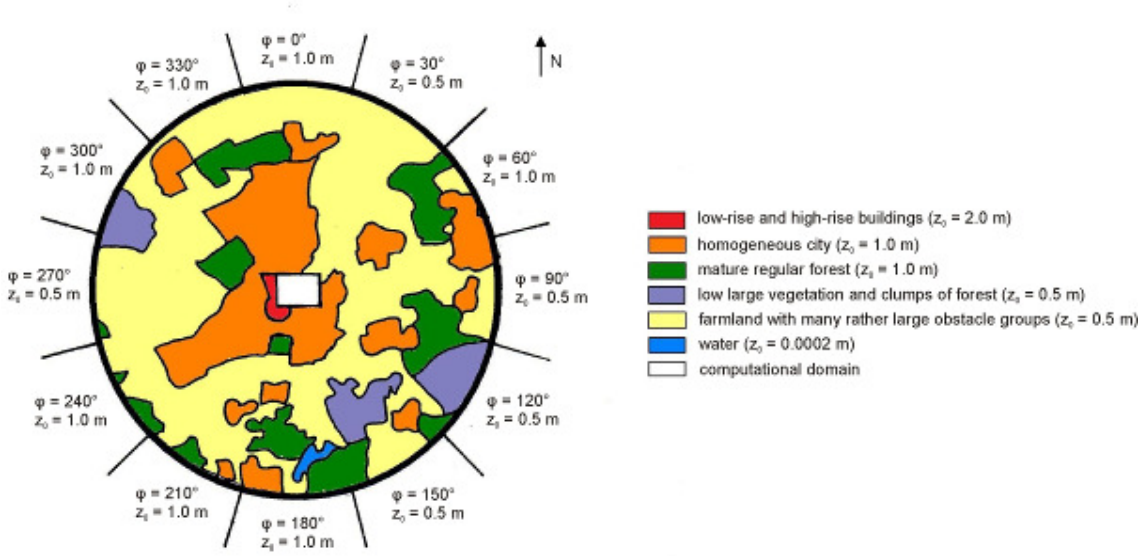

Figure 7. Surroundings of the TU/e campus in a 10 km radius to determine the aerodynamic roughness length z_0 according to the updated Davenport roughness classification. z_0 is determined for every 30° interval. The computational domain used in this study is indicated by the white rectangle.

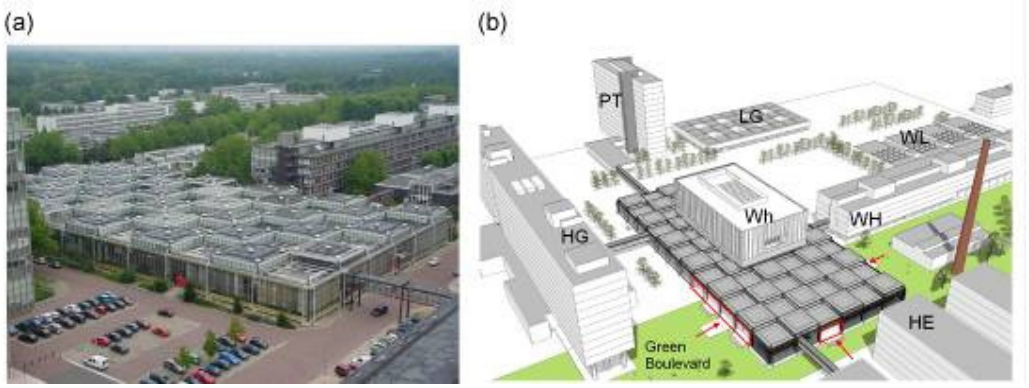

Figure 8. View at W-hall from south-west direction: (a) old situation and (b) new design with addition of high-rise construction and open plaza (courtesy of Ector Hoogstad Architects). The figure also indicates the new Green Boulevard and the west, south and east openings of the roof-covered plaza.

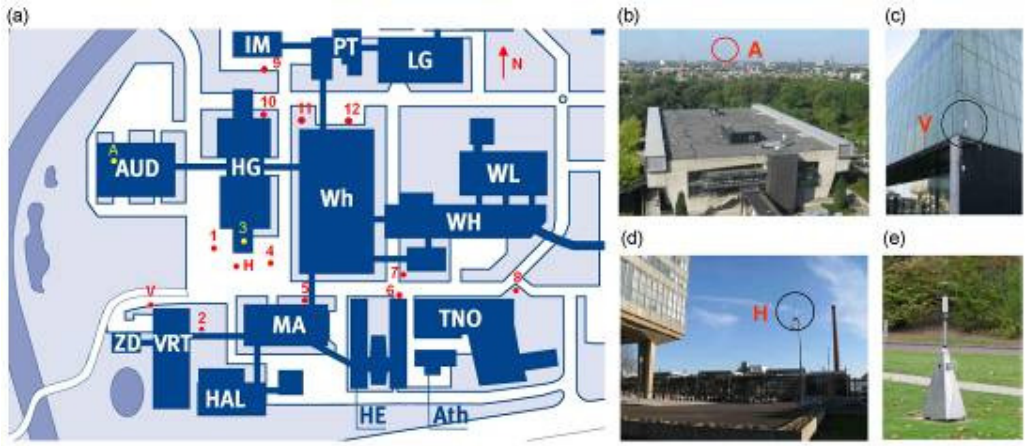

Figure 9. (a) Measurement positions at the campus: The fixed measurement positions A, V and H are at a height of 44.6 m, 5.4 m and 8.9 m. All other positions are mobile positions at pedestrian height, i.e. 1.75 m above ground level. (b-c) Photographs of measurement positions A, V and H. (e) Photograph of mobile measurement station.

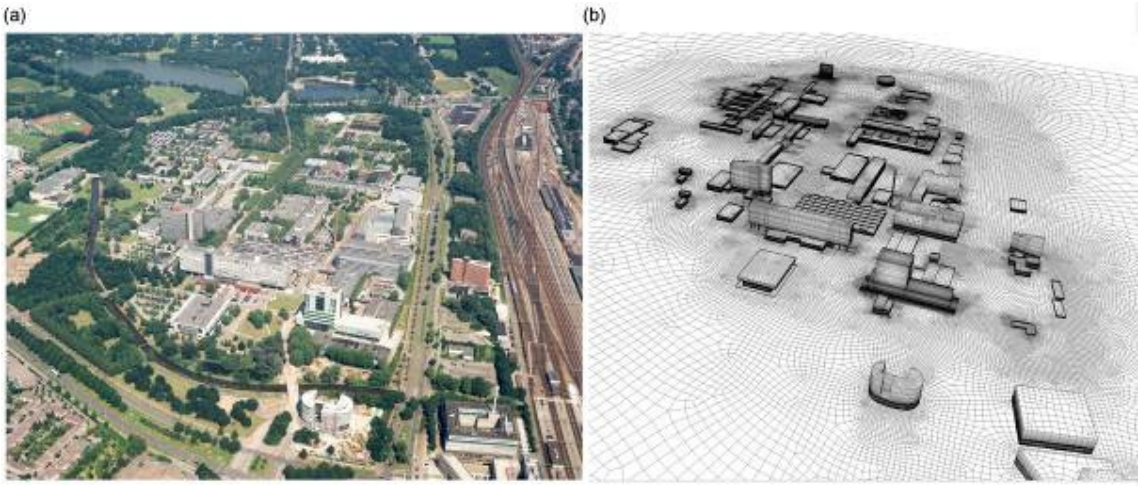

Figure 10. (a) Aerial view of the TU/e campus terrain from southwest. (b) Corresponding high-resolution computational grid (7.554.091 cells). The grid does not include the vegetative elements.

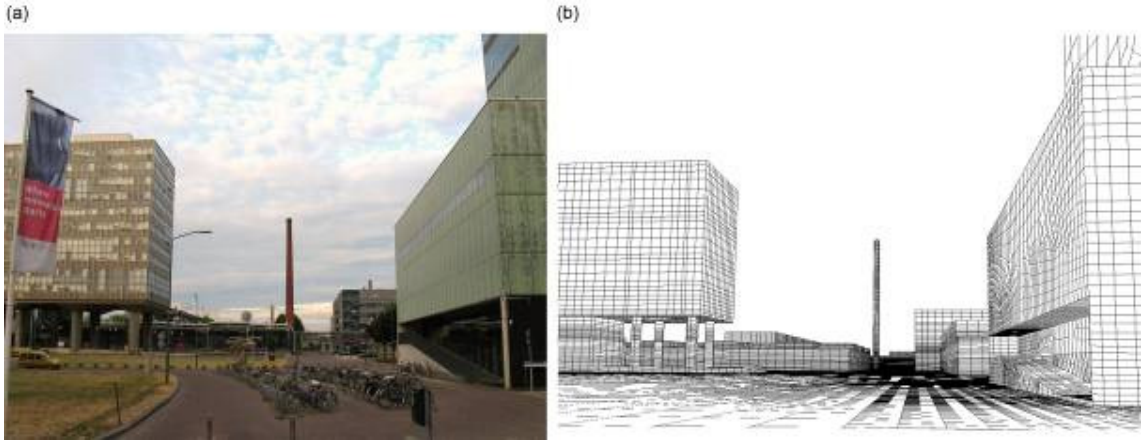

Figure 11. (a) Photo of the TU/e campus terrain from west, with Main Building (HG; left) and Vertigo building (VRT; right). (b) Corresponding high-resolution computational grid (7.554.091 cells).

Figure 12. Roughness specification for the ground surface and for the building surfaces, based on either the aerodynamic roughness length z_0 or the combination of sand-grain roughness height k_S and roughness constant C_S.

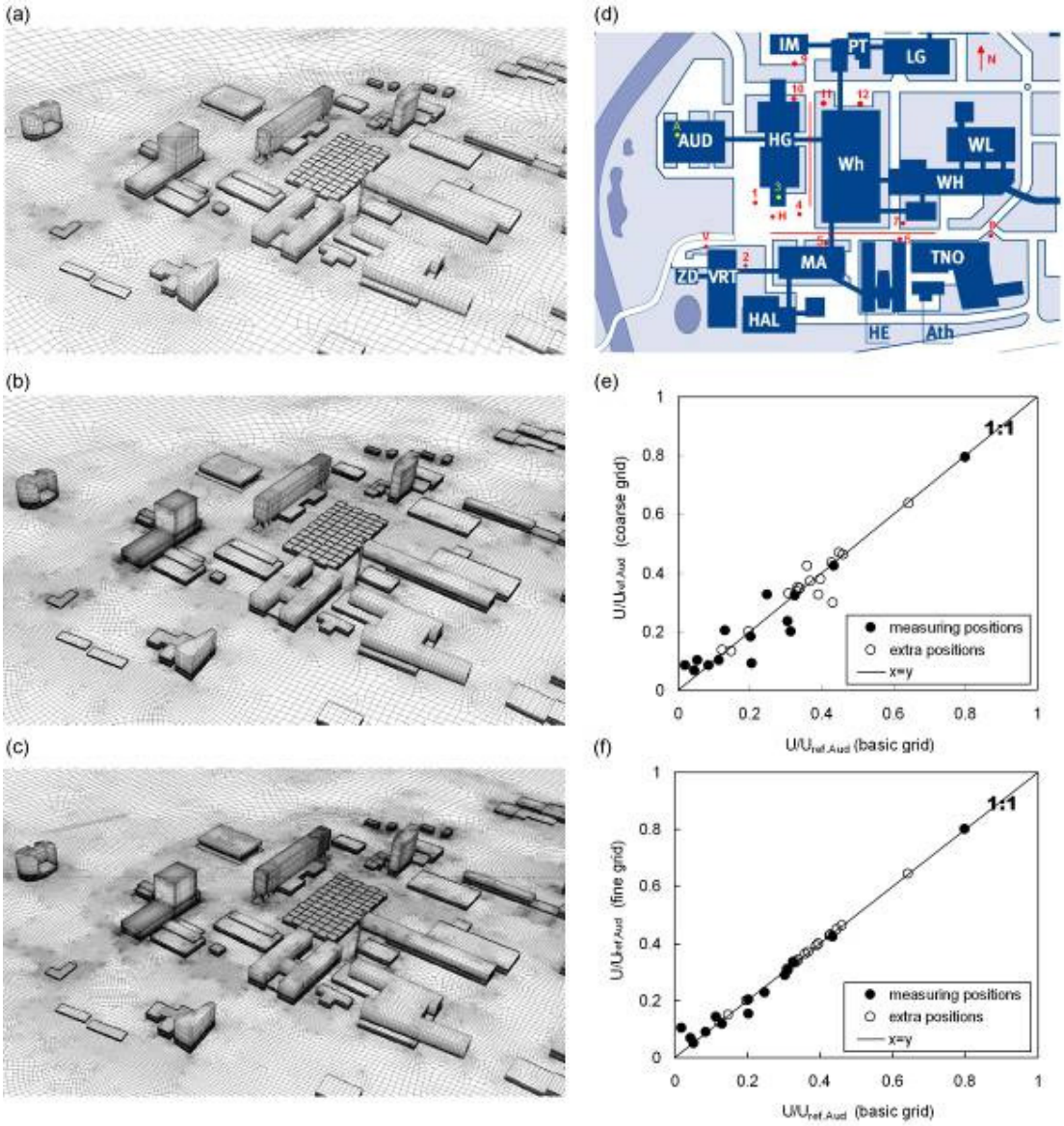

Figure 13. Grid-convergence analysis: (a) Coarse computational grid (2.598.602 cells); (b) Basic grid (7.554.091 cells); (c) Fine grid (12.392.255 cells); (d) Indication of evaluation points and evaluation lines; (e) Comparison of wind speed ratio for coarse and basic grid at evaluation positions; (f) Same for basic and fine grid.

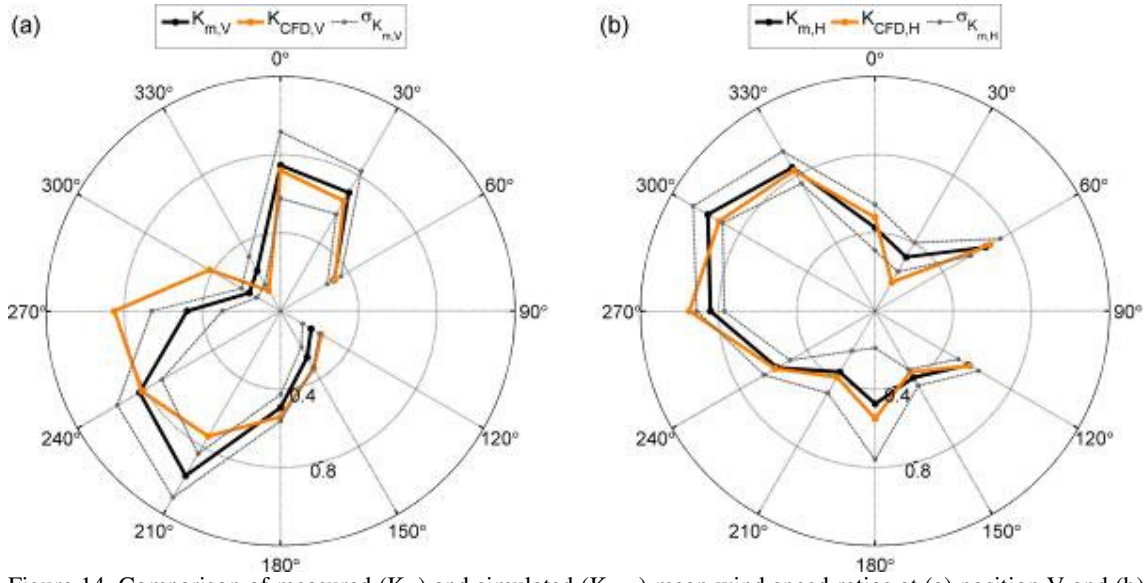

Figure 14. Comparison of measured (K_m) and simulated (K_{CFD}) mean wind speed ratios at (a) position V and (b) position H, for 12 reference wind directions φ_A. The standard deviation of the measurements is also indicated.

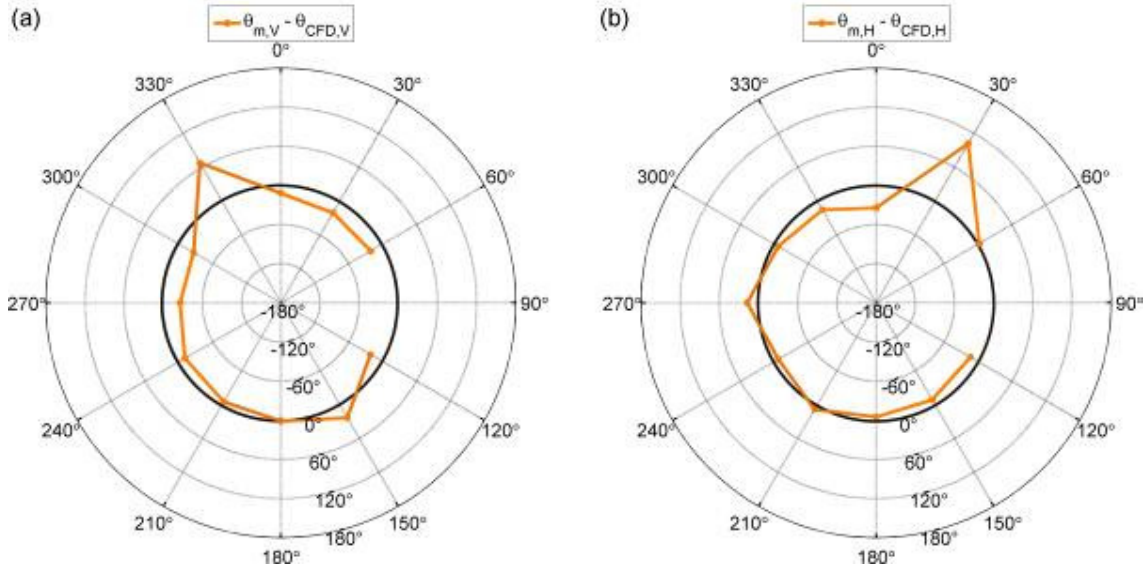

Figure 15. Comparison of measured and simulated local wind directions θ at (a) position V and (b) position H, for 12 reference wind directions φ_A.

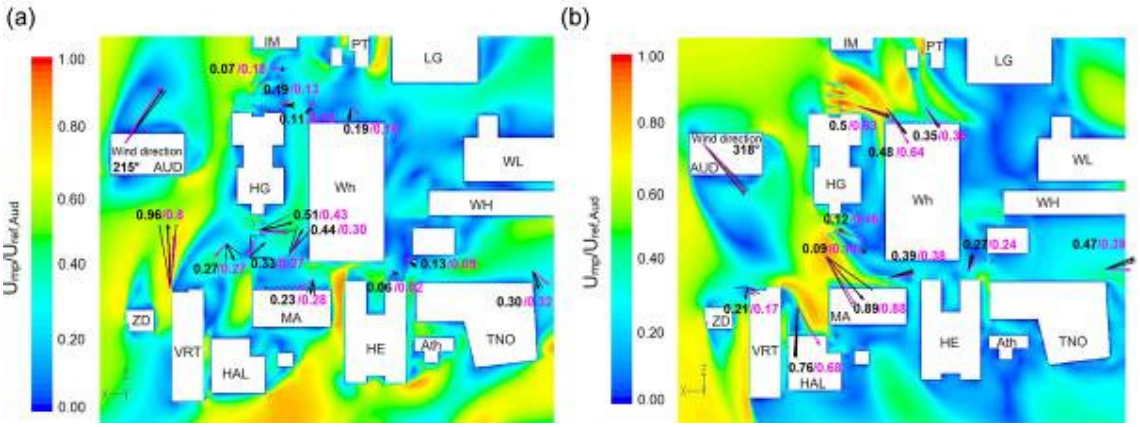

Figure 16. Comparison of simulated and measured mean wind speed ratios and wind directions for two reference wind directions: (a) $\varphi_A = 215°$ and (b) $\varphi_A = 318°$. The vectors and numbers indicate the magnitude of the wind speed ratio.

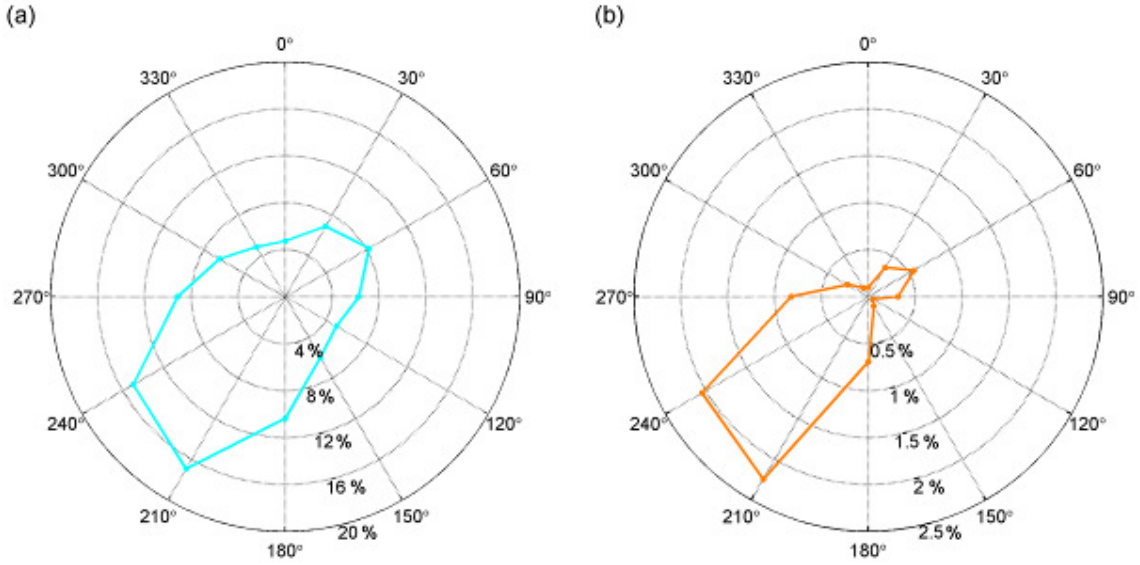

Figure 17. Wind roses for Eindhoven University campus. (a) Standard wind rose with frequency distribution of the hourly mean wind speed. (b) Wind rose with exceedance probability of the 5 m/s threshold at pedestrian height of 1.75 m, based on virtual open field conditions with $z_0 = 0.03$ m..

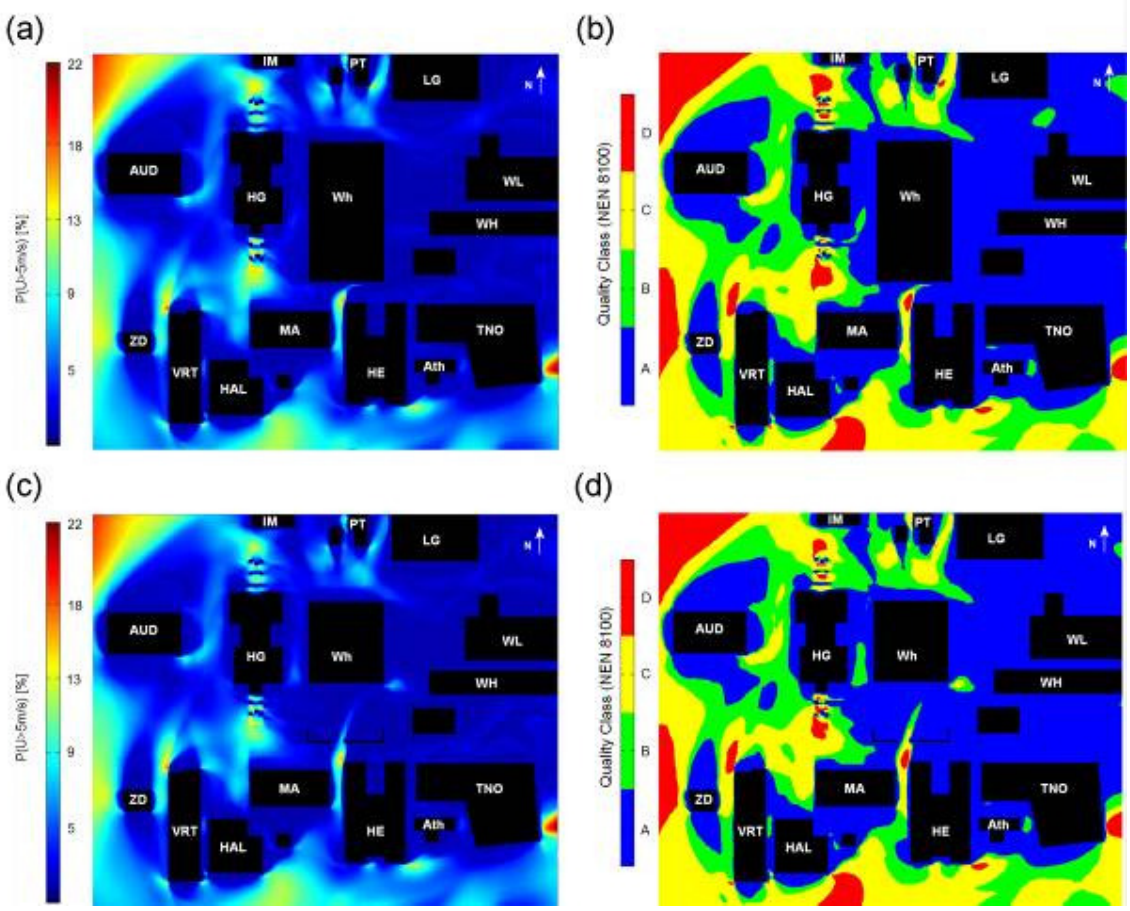

Figure 18. (a) Exceedence probability for wind nuisance at pedestrian level (1.75 m) for the current situation; (b) Corresponding wind comfort quality classes; (c) Same as (a), but for new W-hall design (with roof-covered plaza); (d) Same as (b), but for new W-hall design (with roof-covered plaza).

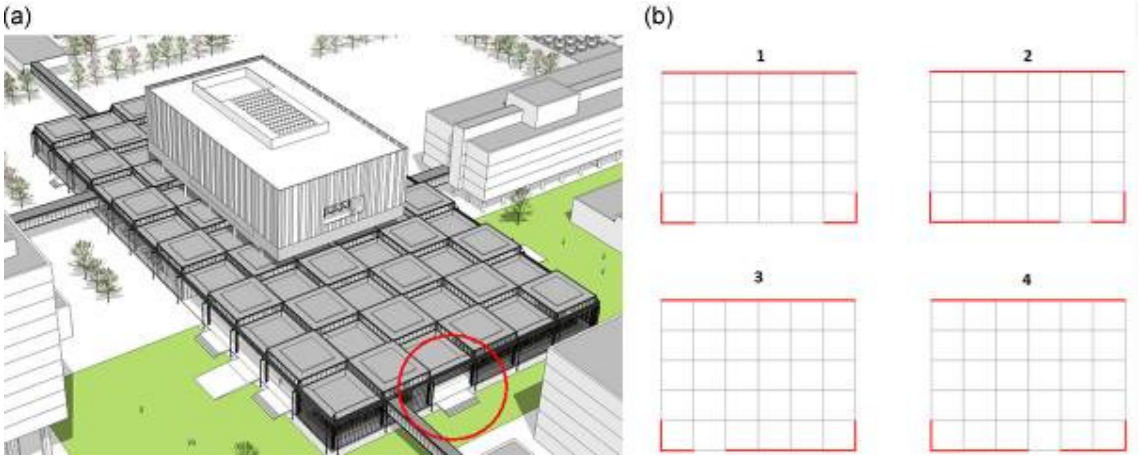

Figure 19. (a) Perspective view of original design of the W-hall and south entrance. (b) Top view of four alternative entrance configurations. The gray/light framed squares show the roof pattern while the red/dark lines show the position of the walls around the plaza.

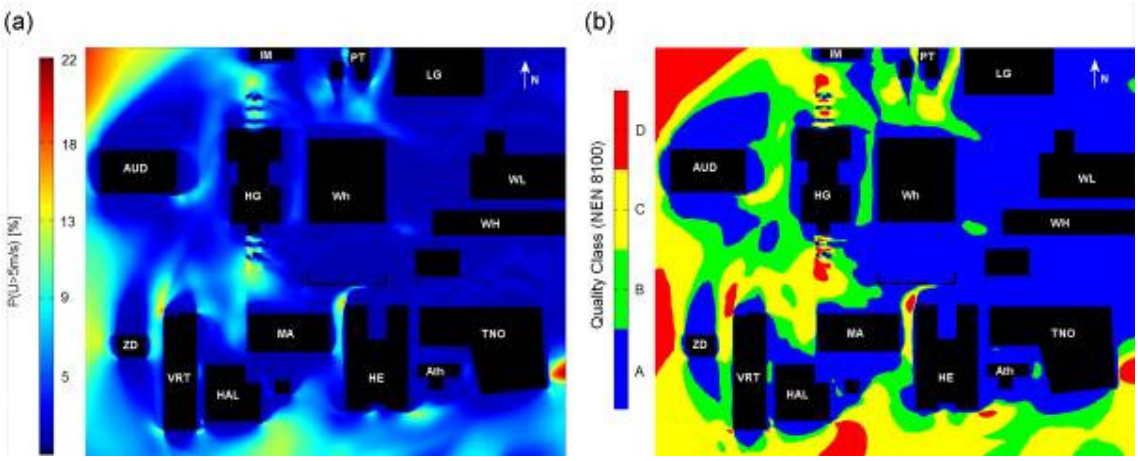

Figure 20 (a) Exceedence probability for wind nuisance at pedestrian level (1.75 m) for the alternative entrance design (option 2 in Fig. 19b); (b) Corresponding wind comfort quality classes according to NEN 8100: the whole plaza has quality class A (good).